

Aldasoro, Iñaki; Gatti, Domenico Delli; Faia, Ester

Working Paper

Bank Networks: Contagion, Systemic Risk and Prudential Policy

CESifo Working Paper, No. 5182

Provided in Cooperation with:

Ifo Institute – Leibniz Institute for Economic Research at the University of Munich

Suggested Citation: Aldasoro, Iñaki; Gatti, Domenico Delli; Faia, Ester (2015) : Bank Networks: Contagion, Systemic Risk and Prudential Policy, CESifo Working Paper, No. 5182, Center for Economic Studies and ifo Institute (CESifo), Munich

This Version is available at:

<https://hdl.handle.net/10419/107350>

Standard-Nutzungsbedingungen:

Die Dokumente auf EconStor dürfen zu eigenen wissenschaftlichen Zwecken und zum Privatgebrauch gespeichert und kopiert werden.

Sie dürfen die Dokumente nicht für öffentliche oder kommerzielle Zwecke vervielfältigen, öffentlich ausstellen, öffentlich zugänglich machen, vertreiben oder anderweitig nutzen.

Sofern die Verfasser die Dokumente unter Open-Content-Lizenzen (insbesondere CC-Lizenzen) zur Verfügung gestellt haben sollten, gelten abweichend von diesen Nutzungsbedingungen die in der dort genannten Lizenz gewährten Nutzungsrechte.

Terms of use:

Documents in EconStor may be saved and copied for your personal and scholarly purposes.

You are not to copy documents for public or commercial purposes, to exhibit the documents publicly, to make them publicly available on the internet, or to distribute or otherwise use the documents in public.

If the documents have been made available under an Open Content Licence (especially Creative Commons Licences), you may exercise further usage rights as specified in the indicated licence.



Working Papers

www.cesifo.org/wp

Bank Networks: Contagion, Systemic Risk and Prudential Policy

Iñaki Aldasoro
Domenico Delli Gatti
Ester Faia

CESIFO WORKING PAPER NO. 5182
CATEGORY 7: MONETARY POLICY AND INTERNATIONAL FINANCE
JANUARY 2015

An electronic version of the paper may be downloaded

- *from the SSRN website:* www.SSRN.com
- *from the RePEc website:* www.RePEc.org
- *from the CESifo website:* www.CESifo-group.org/wp

Bank Networks: Contagion, Systemic Risk and Prudential Policy

Abstract

We present a network model of the interbank market in which optimizing risk averse banks lend to each other and invest in non-liquid assets. Market clearing takes place through a tâtonnement process which yields the equilibrium price, while traded quantities are determined by means of a matching algorithm. We compare three alternative matching algorithms: maximum entropy, closest matching and random matching. Contagion occurs through liquidity hoarding, interbank interlinkages and fire sale externalities. The resulting network configurations exhibits a core-periphery structure, dis-assortative behavior and low clustering coefficient. We measure systemic importance by means of network centrality and input-output metrics and the contribution of systemic risk by means of Shapley values. Within this framework we analyze the effects of prudential policies on the stability/efficiency trade-off. Liquidity requirements unequivocally decrease systemic risk but at the cost of lower efficiency (measured by aggregate investment in non-liquid assets); equity requirements tend to reduce risk (hence increase stability) without reducing significantly overall investment.

JEL-Code: E430, E440, G110, G210, G280.

Keywords: banking networks, centrality metrics, systemic risk.

Iñaki Aldasoro
Goethe University Frankfurt & SAFE
Frankfurt / Germany
aldasoro@safe.uni-frankfurt.de

Domenico Delli Gatti
Catholic University of Milan
Milan / Italy
domenico.delligatti@unicatt.it

Ester Faia
Goethe University Frankfurt, CFS & SAFE
Frankfurt / Germany
faia@wiwi.uni-frankfurt.de

December 2014

For helpful comments we thank participants at the Isaac Newton Institute for Mathematical Sciences Workshop “Regulating Systemic Risk: Insights from Mathematical Modeling”, Cambridge Center for Risk Studies conference on “Financial Risk and Network Theory”, Bundesbank/ESMT/DIW/CFS conference “Achieving Sustainable Financial Stability”, European Economic Association Meetings 2014, Chicago Meeting Society for Economic Measurement 2014, ECB Macro-prudential Research Network Conference, FIRM Research Conference 2014, Unicredit Workshop at Catholic University in Milan “Banking Crises and the Real Economy” and DFG Workshop on “Financial Market Imperfections and Macroeconomic Performance”. We also thank Christoph Roling for helpful comments and suggestions. Parts of this research have been supported by the Frankfurt Institute for Risk Management and Regulation (FIRM). Aldasoro and Faia gratefully acknowledge research support from the Research Center SAFE, funded by the State of Hessen initiative for research LOEWE. Delli Gatti gratefully acknowledges financial support from the FP7 SSH project RASTANEWS (Macro-Risk Assessment and Stabilization Policies with New Early Warning Signals).

1 Introduction

The propagation of bank losses which turned a shock to a relatively small segment of the US financial system (the sub-prime mortgage market) into a large global banking crisis in 2007-2008 is due to a large extent to the increasing number and multifaceted nature of bank interlinkages. Three channels were primarily responsible for this phenomenon of contagion: direct cross-exposures in interbank markets, fire sales externalities and liquidity hoarding due to precautionary banks' behavior. The chain of events can be depicted as follows. As one or more banks are hit by a shock to assets, they find themselves unable to fulfill their debt obligations in the interbank market. Since banks are highly interconnected through borrowing/lending relations, debt defaults inflict losses to many counterparts. Next, as risk averse banks become worried about cascading losses they tend to hoard liquidity. The freeze in interbank liquidity in turn exacerbates banks' inability to honor debts, thereby reinforcing loss propagation. At last, losses force banks to sell non-liquid assets both to re-balance portfolios and to meet equity requirements (and/or VaR constraints). In this way liquidity spirals turn into insolvency and fire sales, which eventually affect the market value of banks' assets. Asset commonality coupled with mark-to-market accounting imply that fire sales inflict balance sheet losses to other banks.¹ Against this background prudential regulators and supervisors are increasingly challenged with a trade off between reducing systemic risk and fostering investment in long term assets.

We lay down a banking network model of the interbank market that captures the channels described above and replicates topological properties of the empirical counterparts (core-periphery structure, low density, dis-assortative behavior). The model consists of N *risk averse* heterogeneous banks which perform optimizing portfolio decisions constrained by VaR (or regulatory) and liquidity requirements. The convexity in the optimization problem generates precautionary liquidity hoarding in face of large shocks. The emerging liquidity freeze contributes to exacerbate loss propagation.² Banks invest in non-liquid assets, which trade at common prices, hence fire sale externalities emerge. Our banks also trade debt contracts with each other in the interbank market, hence defaults and debt interlinkages contribute to loss propagation. Markets are defined by a price vector and a procedure to matching trading partners. The equilibrium price vector (in both the interbank and non-liquid asset markets) is reached through a tâtonnement process,³ in which prices are endogenously determined by sequential convergence of excess demand and supply. Once prices are determined, actual trading among heterogeneous banks takes place through a matching algorithm (see [Gale and Shapley \(1962\)](#) and [Shapley and Shubik \(1972\)](#)). We analyze three alternative algorithms: maximum entropy, closest matching (or minimum distance) and random matching with

¹Fire sales are akin to pecuniary externalities as they work through changes in market prices. See also [Greenwald and Stiglitz \(1986\)](#) and [Mas-Colell et al. \(1995\)](#), chapter 11.

²See also [Afonso and Shin \(2011\)](#).

³See also [Cifuentes et al. \(2005\)](#), [Bluhm et al. \(2013\)](#), [Duffie and Zhu \(2011\)](#).

loading factor. The comparison of the three algorithms is useful for two reasons. First, as stressed in [Shapley and Shubik \(1972\)](#), alternative matching algorithms capture different institutional trading environments. Second, they deliver different network structures and allow us to compare their respective topology, concentration and stability properties.

The rationale for including different channels in our model is twofold. First, several papers⁴ have shown that credit interlinkages and fire sale externalities are not able to produce large contagion effects if taken in isolation. We take both channels into consideration at the same time and – on top of that – we also envisage a third channel, namely liquidity hoarding. Our banking network has also two additional strengths. First, we do not adopt the convention often used in network models according to which links among nodes are exogenous (and probabilistic) and nodes’ behavior is best described by heuristic rules. On the contrary, we adopt the well established economic methodology according to which agents are optimizing, decisions are micro-founded and the price mechanism is endogenous. Second, the baseline configuration of our network model replicates well a number of stylized empirical facts characterizing banking networks.⁵ First of all, in our model banks can be both borrowers and lenders at the same time. Second, our network is characterized by a core-periphery structure, dis-assortative behavior and a low clustering coefficient. Moreover, under certain matching algorithms also the degree of connectivity is low.

We put the model to test to address the role of prudential policy. First, we assess the contribution of each bank to overall risk. This is a crucial aspect of the inspecting activity that any supervisor conducts for crises prevention. We measure banks’ contribution to risk primarily through Shapley values⁶, but we also compare the ranking of systemically important banks using alternative metrics (network centrality and input-output measures).⁷ Generally speaking we find a strong connection between Shapley values and banks’ assets (borrowing and non-liquid assets). High interbank borrowing increases the scope of risk transmission through direct debt linkages. Investment in non-liquid assets enlarges the scope of fire sale externalities. Second, we analyze the impact of changes in regulatory requirements on systemic risk and banks’ contribution to it. Interestingly we find that an increase in the liquidity requirement reduces systemic risk more sharply and more rapidly than an increase in equity requirements. As banks are required to hold more liquidity, they reduce their exposure in the interbank market as well as their investment in non-liquid assets in absolute terms. The fall in interbank supply produces an increase in the interbank interest rate, which, due to asset substitution, induces a fall in non-liquid asset investment relatively to interbank lending. Overall banks become less interconnected in the interbank market and less exposed to swings in the price of

⁴See for instance [Caccioli et al. \(2014\)](#) or [Glasserman and Young \(2014\)](#).

⁵For a recent summary including further references see [Langfield and Soramäki \(2014\)](#).

⁶The Shapley value has been borrowed from the literature on both cooperative and non-cooperative games. See [Shapley \(1953\)](#) and [Gul \(1989\)](#) respectively, and [Drehmann and Tarashev \(2011\)](#) and [Bluhm et al. \(2013\)](#) for applications to banking.

⁷See also [Alves et al. \(2013\)](#) for network centrality metrics. Input-output-based measures are proposed in [Aldasoro and Angeloni \(2014\)](#).

non-liquid assets. Both channels of contagion (cross-exposures and fire sale externalities) become less active. With an increase in the equity requirement instead the demand of interbank borrowing falls and so does the interbank rate. Banks substitute interbank lending, which has become less profitable, with investment in non-liquid assets. While the scope of network externalities and cascades in debt defaults falls, the scope of pecuniary externalities enlarges. On balance systemic risk, and the contribution of each bank to it, declines, but less than with an increase in liquidity requirements.

The rest of the paper is structured as follows. Section 2 relates our paper to the literature. Section 3 describes the model. Section 4 presents the baseline network topology and discusses the empirical matching. Section 5 analyzes the response of the network model to shocks and the contribution of each bank to systemic risk. Section 6 focuses on the policy analysis. Section 7 concludes. Appendices with figures and tables follow.

2 Related Literature

After the collapse of Lehman and the worldwide spreading of financial distress two views have emerged regarding the mechanisms triggering contagion. According to the first one, cascading defaults are due to credit interconnections. In high value payment systems banks rely on incoming funds to honor payments of outflows; when synchronicity breaks down and banks fail to honour debts, cascading defaults emerge. Eisenberg and Noe (2001), Afonso and Shin (2011) or Elliott et al. (2014) analyze this channel using lattice-theoretic methods to solve for the unique fixed point of an equilibrium mapping. Works in this area take the payment relations as given: we make a step forward as credit interlinkages in our model result from portfolio optimization and endogenous price mechanisms.⁸ According to the second view financial distress is triggered by fire sale externalities in environments characterized by asset commonality coupled with mark-to-market accounting. As one bank is hit by a shock, it tries to sell assets to meet VaR or capital constraints. Under mark-to-market accounting, the endogenous fall in market prices negatively affects other banks' balance sheets. Cifuentes et al. (2005) and Bluhm et al. (2013) also formalize this mechanism. Our model encompasses both views and shows that both are important to account for risk propagation. Moreover, we bring to the fore a third mechanism based on liquidity hoarding: once financial distress has emerged banks become more cautious and hoard liquidity. The ensuing liquidity freeze amplifies risk propagation. A similar channel is present also in Afonso and Shin (2011).

Our paper is also related to three other strands of recent literature. First, it contributes to the literature which tries to assess the trade-offs between risk sharing and risk propagation. Using an interbank network modelled as a credit chain, Allen and Gale (2000) show the existence of

⁸See also Bluhm et al. (2013) and Halaj and Kok (2014).

a monotonically decreasing relation between systemic risk and the degree of connectivity.⁹ More recent views challenge - at least in part - this conclusion by showing that a *trade off* emerges between decreasing individual risk due to risk sharing and increasing systemic risk due to the amplification of financial distress. Battiston et al. (2012) show for instance that the relation between connectivity and systemic risk is hump shaped: at relatively low levels of connectivity, the risk of individual default goes down with density thanks to risk sharing while at high levels of connectivity, a positive feedback loop makes a bank under distress more prone to default as the number of partners under distress increases.¹⁰ In the numerical simulations of our model, we will assume a multinomial distribution of correlated shocks in order to capture the presence of feedback loops.

Secondly, our paper is related to the literature analyzing metrics of systemic risk and measuring the contribution of each bank to it. We make a more extensive overview of those papers and their relation to ours in the next section and in Appendix D. Third, a connection can also be established with the literature analyzing matching mechanisms in markets along the lines indicated by Shapley and Shubik (see for instance Shapley and Shubik (1972)). Finally, our paper is related to an emerging literature studying prudential regulation in financial networks (see for instance Gai et al. (2011)).

3 The Banking Network

We consider a financial system consisting of N banks, each one represented by a node. For this population of banks we can define ex-ante a network $g \in G$ as the set of links (borrowing/lending relationships) where G represents the set of all possible networks. The network is weighted: an edge or link between banks i and j is indicated by the element $g_{ij} \in \mathbb{R}$ where g_{ij} represents the amount (in money) lent by bank i to bank j . Moreover, the network is directed i.e. $g_{ij} \neq g_{ji}$, $i \neq j$. Notice that each bank can be both a borrower and a lender vis-à-vis different counterparties. An important aspect is that cross-lending positions (hence the network links) result endogenously from the banks' optimizing decisions (see next section) and the markets' tâtonnement processes. Banks in our model are characterized also by external (non interbank) assets (cash and non-liquid assets) and liabilities (deposits). As usual, equity or net worth is defined as the difference between total assets and total liabilities. By assumption, banks are heterogenous due to different returns on non-liquid assets.¹¹

Prices in the interbank market and the market for non-liquid assets are determined by a se-

⁹In their model each bank is linked only to one neighbor along a ring. They show that the probability of a bankruptcy avalanche is equal to one in the credit chain, but that, as the number of partners of each bank increases (namely when the credit network becomes complete), the risk of individual default goes asymptotically to zero due to the improved risk sharing possibilities.

¹⁰Also Gai et al. (2011) derive a non-monotonic relationship between connectivity and systemic risk.

¹¹In the numerical simulation we will also allow the model to account for heterogeneity in the level of deposits and equities.

quential tâtonnement processes. In the first stage of the sequence, clearing takes place in interbank market, given the price of non-liquid assets. In the second stage clearing takes place in the market for non-liquid assets. In each market walrasian auctioneers (see also Cifuentes et al. (2005) or Duffie and Zhu (2011)) receive individual demand and supply (of interbank loans and of non liquid assets respectively) and adjust prices¹² until the distance between aggregate demand and supply has converged to zero.¹³ Once a clearing price has been achieved, actual trade takes place. Traded quantities in our model are determined according to three different matching mechanisms: maximum entropy, closest matching and random matching (see Section 3.2.2 for details).

A general overview of the model and the channels which operate in it are described visually in Appendix B.

3.1 The banking problem

Our network consists of optimizing banks which solve portfolio optimization problems subject to regulatory and balance sheet constraints. Banks are risk averse and have convex marginal utilities. The convex optimization problem (concave objective function subject to linear constraints) allows us to account for interior solutions for both borrowing and lending. Banks are therefore on both sides of the interbank market vis-à-vis different counterparties: this feature is a necessary condition for a core-periphery configuration to emerge. Furthermore we assume that banks have concave marginal utilities with respect to profits.¹⁴ Empirical observation shows that banks tend to adopt precautionary behavior in an uncertain environment.¹⁵ Convex marginal utilities allow us to account for this fact, since in this case banks' expected marginal utility (hence banks' precautionary savings) tends to increase with the degree of uncertainty.

Banks' portfolios are made up of cash, non-liquid assets and interbank loans. Moreover, banks are funded by means of deposits and interbank loans. Hence, the balance sheet of bank i is given by:

$$c_i + pn_i + \underbrace{l_{i1} + l_{i2} + \dots + l_{ik}}_{\equiv l_i} = d_i + \underbrace{b_{i1} + b_{i2} + \dots + b_{ik'}}_{\equiv b_i} + e_i \quad (1)$$

where c_i represents cash holdings, n_i denotes the volume and p the price of non liquid assets (so that pn_i is the market value of the non liquid portion of the bank's portfolio), d_i stands for deposits and e_i for equity. l_{ij} is the amount lent to bank j where $j = 1, 2, \dots, k$ and k is the

¹²As in all centralized tâtonnement processes this adjustment takes place in fictional time with no actual trading. Trading takes place only when price convergence has been achieved.

¹³Banks in our model are risk averse, hence have concave objective functions and linear constraints. The convexity of the optimization problem and the assumption of an exponential aggregate supply function guarantees that individual and aggregate excess demand and supplies behave in both markets according to Liapunov convergence.

¹⁴This amounts to assuming a positive third derivative.

¹⁵See also Afonso and Shin (2011).

cardinality of the set of borrowers from the bank in question; b_{ij} is the amount borrowed from bank j where $j = 1, 2, \dots, k'$ and k' is the cardinality of the set of lenders to the bank in question. Hence $l_i = \sum_{j=1}^k l_{ij}$ stands for total interbank lending and $b_i = \sum_{j=1}^{k'} b_{ij}$ stands for total interbank borrowing.¹⁶

The bank's optimization decisions are subject to two standard regulatory requirements:

$$c_i \geq \alpha d_i \quad (2)$$

$$er_i = \frac{c_i + pn_i + l_i - d_i - b_i}{\omega_n pn_i + \omega_l l_i} \geq \gamma + \tau \quad (3)$$

Equation 2 is a liquidity requirement according to which banks must hold at least a fraction α of their deposits in cash. Equation 3 is an equity requirement (which could also be rationalized as resulting from a VaR internal model). It states that the ratio of equity at market prices (at the numerator) over risk weighted assets (at the denominator) must not fall below a threshold $\gamma + \tau$. Cash enters the constraint with zero risk weight since it is riskless in our model, while ω_n and ω_l represent the risk weights on non-liquid assets and interbank lending respectively. The parameter γ is set by the regulator, while the parameter τ captures an additional desired equity buffer that banks choose to hold for precautionary motives.

The bank's profits are given by the returns on lending in the interbank market (at the interest rate r^l) plus returns from investments in non-liquid assets (whose rate of return is r_i^n) minus the expected costs from interbank borrowing.¹⁷ The rate of return on non-liquid assets is exogenous and heterogeneous across banks: we assume that banks have indeed access to investment opportunities with different degrees of profitability. The interest rates on borrowed funds are also heterogeneous across banks due to a risk premium. In lending to j , bank i charges a premium r_j^p over the risk-free interest rate (i.e. the interest rate on interbank loans r^l), which depends on the probability of default of j , pd_j . The premium can be derived through an arbitrage condition. By lending l_{ij} to j , bank i expects to earn an amount given by the following equation:

$$\underbrace{(1 - pd_j) (r^l + r_j^p) l_{ij}}_{\text{with no default}} + \underbrace{pd_j (r^l + r_j^p) (1 - \xi) l_{ij}}_{\text{with default}} \quad (4)$$

where ξ is the loss given default parameter. When bank j does not default, bank i gets:

$$l_{ij} r^l \quad (5)$$

By equating 4 and 5 we can solve for the fair risk premium charged to counterparty j :

¹⁶Note that since banks cannot lend to nor borrow from themselves, we set $l_{ii} = b_{ii} = 0 \forall i = 1, \dots, N$.

¹⁷For simplicity it is assumed that deposits are not remunerated.

$$r_j^p = \frac{\xi p d_j}{1 - \xi p d_j} r^l \quad (6)$$

It is immediate to verify that the premium is calculated so that, by lending to j , bank i expects to get $r^l l_{ij}$ (to obtain this, plug the premium back into 4). We can interpret condition 4 also as a participation constraint: bank i will lend to bank j only if it gets an expected return from lending equal to the risk free rate, i.e. the opportunity cost of lending. By summing up over all possible counterparties of bank i , and recalling that $l_i = \sum_{j=1}^k l_{ij}$, we retrieve the overall gain that bank i expects to achieve by lending to all the borrowers: $r^l l_i$. On the other hand, as a borrower bank i must also pay the premium associated to its own default probability.¹⁸ Therefore the cost of borrowing is given by: $r_i^b b_i = (r^l + r_i^p) b_i = \frac{1}{1 - \xi p d_i} r^l b_i$.

Finally, the gains from investment in non-liquid assets are given by: $r_i^n \frac{n_i}{p}$. In what follows we will assume that the price of non-liquid assets is set to $p = 1$ so the last expression simplifies to $r_i^n n_i$. Given these assumptions, the profits of bank i read as follows:

$$\pi_i = r_i^n n_i + r^l l_i - (r^l + r_i^p) b_i = r_i^n n_i + r^l l_i - \frac{1}{1 - \xi p d_i} r^l b_i \quad (7)$$

The bank's preferences are represented by a CRRA utility function:

$$U(\pi_i) = \frac{(\pi_i)^{1-\sigma}}{1-\sigma} \quad (8)$$

where σ stands for the bank's risk aversion. As explained above the convex maximization problem serves a dual purpose. First, it allows us to obtain interior solutions for borrowing and lending. Second, since the CRRA utility function is characterized by convex marginal utilities (positive third derivatives), we can introduce banks' precautionary behavior in the model. As marginal utilities are convex with respect to profits, higher uncertainty induces higher expected marginal utility at the optimal point. As expected marginal utility increases banks tend to be more cautious and to hoard liquidity.

With concave utility, uncertainty regarding debt repayment makes variance about returns affect the bank's decision. In this set up it is convenient to take a second order Taylor approximation of the expected utility of profits. Details of the derivation of the objective function of banks can be found in [Appendix A](#). The approximated objective function is therefore given by:

$$E[U(\pi_i)] \approx \frac{E[\pi_i]^{1-\sigma}}{1-\sigma} - \frac{\sigma}{2} E[\pi_i]^{-(1+\sigma)} \left(n_i^2 \sigma_{r_i^n}^2 - (b_i r^l)^2 \xi^2 (1 - \xi E[p d_i])^{-4} \sigma_{p d_i}^2 \right) \quad (9)$$

¹⁸Since banks charge a fair risk premium, the returns that banks obtain from non-defaulting borrowers offset the losses resulting from contracts with defaulting borrowers. Borrowing banks, on the other hand, must always pay the premium.

where $E[\pi_i]$ stands for expected profits while $\sigma_{r_i^n}^2$ and $\sigma_{pd_i}^2$ stand for the variances of returns on non-liquid assets and default probability respectively. The problem of bank i can be summarized as:

$$\begin{aligned}
& \text{Max}_{\{c_i, n_i, l_i, b_i\}} && E[U(\pi_i)] \\
& \text{s.t.} && \text{Equation 2, Equation 3, Equation 1} \\
& && c_i, n_i, l_i, b_i \geq 0
\end{aligned} \tag{P}$$

3.2 Interbank Market Clearing

The interbank market clears in two stages. In the first stage a standard tâtonnement process is applied (see Mas-Colell et al. (1995)) and the interbank interest rate is obtained by clearing excess demand/supply. Individual demands and supply (as obtained from banks' optimization) are summed up. If an excess demand or supply occurs the interbank rate is adjusted sequentially to clear the discrepancy. In the second stage, after the equilibrium interbank rate has been determined, a matching algorithm determines the actual pairs of banks involved into bilateral trading (at market prices).

3.2.1 Price Tâtonnement in the Interbank Market

For a given calibration of the model, which includes an initial level of the interbank interest rate, the bank chooses the optimal demand (b_i) and supply (l_i) of interbank debt trading. These are submitted to a walrasian auctioneer who sums them up and obtains the market demand $B = \sum_{i=1}^N b_i$ and supply $L = \sum_{i=1}^N l_i$. If $B > L$ there is excess notional demand in the market and therefore r^l is increased, whereas the opposite happens if $B < L$.¹⁹ Changes in the interbank rates are bounded within intervals which guarantee the existence of an equilibrium (see Mas-Colell et al. (1995)). The upper limit of the interval is the highest yield on non-liquid assets, r^l ($\bar{r}_{(0)}^l$), and the lower limit, $\underline{r}_{(0)}^l$, is set to zero. When solving portfolio optimization banks take as given an initial value for the interbank returns which is given by $r_{(0)}^l = \frac{\bar{r}_{(0)}^l + \underline{r}_{(0)}^l}{2}$. To fix ideas imagine that at the initial value banks' optimization yields an aggregate excess supply of interbank lending (i.e. $L > B$). To clear the excess the interbank rate must fall to a new level given by $r_{(1)}^l = \frac{r_{(0)}^l + \underline{r}_{(0)}^l}{2}$; the latter is obtained by setting $\bar{r}_{(0)}^l$ as the new upper bound. Given the new interbank rate a new round of optimization and clearing starts. Notice that in the new round atomistic banks re-optimize by taking as given

¹⁹This iteration normally takes place in fictitious time. Banks do not trade during interest rate adjustment. Trade only occurs once the equilibrium interest rate has been determined.

the new interbank rate $r_{(1)}^l$. This process continues until the change in interest rate is below an arbitrarily small threshold level.²⁰ A similar adjustment is undertaken in the opposite direction if $B > L$.

The clearing price process delivers two vectors, $\mathbf{l} = [l_1 \ l_2 \ \dots \ l_N]$ and $\mathbf{b} = [b_1 \ b_2 \ \dots \ b_N]$, which correspond to optimal lending and borrowing of each bank for given equilibrium prices.

3.2.2 Matching algorithms

Once the equilibrium interest rate has been achieved, actual bilateral trading relations among banks have to be determined. This is to say that given the vectors $\mathbf{l} = [l_1 \ l_2 \ \dots \ l_N]$ and $\mathbf{b} = [b_1 \ b_2 \ \dots \ b_N]$ obtained during the price clearing process we need to match pairs of banks for the actual trading to take place. We will use a matching algorithm to determine how bank i distributes its lending ($l_i = \sum_{j=1}^k l_{ij}$) and/or borrowing ($b_i = \sum_{j=1}^{k'} b_{ij}$) among its potential counterparties.

The matching algorithm, therefore, will determine the structure of the network. We use three alternative algorithms. Each one delivers different topological properties for the resulting network. Our goal is to assess the network topologies generated by these algorithms in terms of (i) comparison with their empirical counterparts, (ii) stability properties and (iii) the relative effectiveness of prudential policy measures.

Mathematically the matching algorithms deliver the matrix of interbank positions \mathbf{X} , with element x_{ij} indicating the exposure (through lending) of bank i to bank j , starting from the vectors \mathbf{l} and \mathbf{b} . Once all trading has been cleared the vectors \mathbf{l} and \mathbf{b} will also correspond to the row sum and column sum (respectively) of the matrix \mathbf{X} .²¹ The algorithms are characterized as follows:

(i) Maximum Entropy. The most common approach to the determination of bilateral trading used in the empirical literature is the maximum entropy method.²² This approach distributes lending and borrowing as evenly as possible among counterparties in conjunction with restrictions on the diagonal elements of the matrix to be estimated. Given the vectors \mathbf{l} and \mathbf{b} , the matrix \mathbf{X} obtained by this method yields the maximum density possible, that is, the market will be as complete as possible in the sense of Allen and Gale (2000). To obtain the maximum entropy solution we follow Drehmann and Tarashev (2011) and employ the RAS algorithm, a technique of bi-proportional matrix balancing developed in the context of input-output analysis for the purpose of matrix updating. The maximum entropy solution uses the data based relative entropy matrix as a prior: this matrix assumes that the exposure of bank i to bank j is given by $x_{ij} = l_i * b_j$ if $i \neq j$ and equal to zero if $i = j$. The strength of this approach lies on the fact that the calibration of the priors is based on actual data. The weakness is that it generates interbank matrices that are

²⁰Equivalently, one can think of the process as stopping when $|L - B| \leq \varepsilon$, where ε is an arbitrarily small threshold.

²¹The generic element x_{ij} of matrix \mathbf{X} is a proxy – generated by the algorithm – of l_{ij} . Generally, each algorithm generates a different proxy. Under all matching algorithms, however, we assume that the diagonal of matrix \mathbf{X} is filled with zeros: by construction banks cannot lend to and borrow from themselves.

²²See for instance Upper (2011) and references therein.

considerably less sparse (more “dense”) than real-world interbank matrices.

(ii) Closest matching (CMA). The second algorithm we employ is the closest matching, or minimum distance, algorithm.²³ The rationale behind this mechanism lies in matching pairs of banks whose desired demand and supply are close in terms of size.²⁴ In this case matching takes place sequentially following the notion of deferred-acceptance established in Gale and Shapley (1962). The interbank trading matrix obtained by this method has considerably lower connectivity than the one obtained via maximum entropy, providing in fact a minimum density matrix. In this respect the model with CMA generates a degree of connectivity close to the one observed in the data. The CMA is also based on a stability rationale, as it is generally compatible with pair-wise efficiency and has been proposed in the seminal treaty of Shubik (1999) as most apt to capture clearing in borrowing and lending relations.

(iii) Random matching with loading factor (RMA). The first two matching mechanisms outlined above generate, respectively, upper and lower bounds in terms of connectivity. We consider also an algorithm which generates an intermediate degree of connectivity and in which partners are matched randomly. In particular, the cell corresponding to the bilateral trading for pairs (i, j) in matrix \mathbf{X} is chosen at random and given by the value $x_{ij} = \lambda \min\{l_i, b_j\}$, where λ is a loading parameter that can be varied and which we set to 0.99 in order to get a density of roughly 22% in the baseline simulation.²⁵ This matching algorithm captures the idea that, should interbank activity result from banks accommodating unexpected random liquidity shocks as in the seminal contribution by Diamond and Dybvig (1983), the interbank market structure would show a random configuration.

3.3 Price Tâtonnement in the Market for Non-Liquid Assets

The clearing process in the market for non-liquid assets is modelled along the lines of Cifuentes et al. (2005). The price of non-liquid assets is initially set to 1. This is the price corresponding to zero aggregate sales and banks fulfilling regulatory requirements. The occurrence of shocks to banks’ non-liquid asset holdings may force them to put some of their stock of assets on the market in order to fulfill regulatory requirements. This increases the supply of assets above demand. As a result the market price adjusts to clear the market.

Given the optimal portfolio decisions, we can denote the bank’s optimal supply (or demand) of non-liquid assets with s_i . Since s_i is decreasing in p , the aggregate sales function, $S(p) = \sum_i s_i(p)$,

²³Bluhm et al. (2013) employ this matching algorithm. In their model however banks are either borrowers or lenders and this simplifies the workings of the algorithm. In our model the algorithm needs to be adapted to allow for banks entertaining multiple borrowing and lending relations.

²⁴Notice that since banks can ex-post differentiate risk premia according to the risk of the borrower, they are effectively indifferent among alternative counterparts. As noted above, risk premia are derived so as to achieve certainty equivalence under the assumption of concave banks’ objectives.

²⁵Notice that the case of $\lambda = 1$ nests an algorithm with minimum density matrix.

is also decreasing in p . An equilibrium price is such that total excess demand equals supply, namely $S(p) = D(p)$. The aggregate demand function $\Theta : [p, 1] \rightarrow [p, 1]$ will be denoted with $\Theta(p)$. Given this function, an equilibrium price solves the following fixed point problem:

$$\Theta(p) = d^{-1}(S(p)) \quad (10)$$

The price at which total aggregate sales are zero, namely $p = 1$, can certainly be considered one equilibrium price. But a key insight from [Cifuentes et al. \(2005\)](#) is that a second (stable) equilibrium price exist to the extent that the supply curve $S(p)$ lies above the demand curve $D(p)$ for some range of values. The convergence to the second equilibrium price is guaranteed by using the following inverse demand function²⁶:

$$p = \exp(-\beta \sum_i s_i), \quad (11)$$

where β is a positive constant to scale the price responsiveness with respect to non-liquid assets sold, and s_i is the amount of bank i 's non-liquid assets sold on the market. Integrating back the demand function in [Equation 11](#) yields the following:

$$\frac{dp}{dt} = \beta S(p) \quad (12)$$

which states that the price will go up (down) in the presence of excess demand (supply). In the above differential equation β represents the rate of adjustment of prices along the dynamic trajectory.

Numerically, price tâtonnement in the market for non-liquid assets takes place through an iterative process which can be described as follows. At the initial equilibrium the price is set to 1. Following a shock to the non-liquid asset portfolio of any given bank, a shift in aggregate supply occurs. Bank i starts selling non-liquid assets to satisfy its equity requirement and this results into $S(1) = s_i > 0$. At $S(1)$ the bid price, given by the inverse demand function, namely [Equation 11](#), is given by $p(S(1))^{bid}$, while the offer price is one. Given this discrepancy the new price is set at the intermediate level between the two, $p(S(1))^{mid}$. The new price is lower than the initial equilibrium price. This determines a fall in the value of banks' non-liquid asset portfolios. Once again to fulfill equity requirements banks are forced to sell assets again, a process which forces further price falls through the mechanism just described. The iterative process continues until demand and supply cross at the equilibrium price p^* . Notice that convergence is guaranteed since we have a downward sloping market demand function given by [Equation 11](#).

²⁶This function can be rationalized by assuming the existence of some noise traders in the market.

3.4 Equilibrium Definition

Definition. A competitive equilibrium in our model is defined as follows:

- (i) A quadruple (l_i, b_i, n_i, c_i) for each bank i that solves the optimization problem P .
- (ii) A clearing price in the interbank market, r^l , which satisfies $B = L$, with $B = \sum_{i=1}^N b_i$ and $L = \sum_{i=1}^N l_i$.
- (iii) A trading-matching algorithm for the interbank market.
- (iv) A clearing price for the market of non-liquid assets, p , that solves the fixed point: $\Theta(p) = d^{-1}(s(p))$.

3.5 Risk Transmission Channels in the Model

Before proceeding with the simulation results, it is useful to highlight the main channels of risk transmission in this model. Overall, there are three channels.

First, a direct channel goes through the lending exposure in the interbank market. When a bank – say bank i – is hit by a shock which makes it unable to repay interbank debt, default losses are transmitted to all the banks exposed to i through interbank loans. Depending on the size of losses, these banks, in turn, might find themselves unable to fulfill their obligations in the interbank market.

The increase of default losses in the presence of risk averse banks also increases their cautiousness, thereby forcing them to hoard liquidity. The ensuing fall in the supply of liquidity amplifies the cascading effects of bank losses. This is the second (indirect) channel of risk transmission.

As borrowing banks find less liquidity available in the market they end up investing less in non liquid assets or might be forced to sell them if they do not meet the regulatory requirements. A third and last channel of losses and risk transmission therefore is a traditional fire sale mechanism that works through pecuniary externalities. The channel, highlighted theoretically by [Greenwald and Stiglitz \(1993\)](#), has been recently modelled within financial networks by [Cifuentes et al. \(2005\)](#). The mechanism in our model works as follows. A bank hit by a shock might be forced to sell non-liquid assets in order to meet equity requirements and/or *VaR* targets. If the sale of the assets is large enough, the market experiences a collapse of the asset price. This is the essence of pecuniary externalities, namely the fact that liquidity scarcity and the ensuing individual banks' decisions have an impact on market prices. In an environment in which banks' balance sheets are measured with mark-to-market accounting, the fall in the asset price induces accounting losses to all banks which have invested in the same asset. Accounting losses force other banks to sell non-liquid assets under distress. This vicious circle contributes to turn a small shock into a spiralling chain of sales and losses. Three elements are crucial in determining the existence of fire sale externalities in our model. First, the presence of equity requirements affects market demand elasticities in a way that individual banks' decisions about asset sales do end up affecting market prices. Second, the

tâtonnement process described above produces falls in asset prices whenever supply exceeds demand. Third, banks' balance sheet items are evaluated with a mark-to-market accounting procedure.

All the above-mentioned channels (credit interconnections among banks, liquidity hoarding and fire sales) have played an important role during the 2007 crisis. [Caballero and Simsek \(2013\)](#) for instance describe the origin of fire sale externalities in a model in which complex financial architecture also induces uncertainty, which amplifies financial panics. [Afonso and Shin \(2011\)](#) instead focus on loss transmission due to direct exposure of banks in the money market and through liquidity hoarding. Our model merges those approaches and gains a full picture of the extent of the cascade following shocks to individual banks²⁷.

The mechanisms just described are in place even if the shock hits a single bank. However to produce a more realistic picture in the simulations presented below we assume a multinomial distribution of shocks to non-liquid assets: initial losses can therefore hit all banks and can also be correlated.

3.6 Systemic Risk and Systemic Importance

One contribution of our paper lies in deriving and comparing various metrics of systemic importance and banks' individual contributions to systemic risk. Importantly, those metrics have so far and most often been derived in networks with non-optimizing agents and without endogenous price formation. Blending those two components is one of the challenges we undertake.

As background it is important to notice that the 2007-8 crisis moved the attention of supervisory authorities from the too-big-to fail to the too-interconnected-to fail banks. In the past, systemically important banks were identified based on concentration indices such as the Herfindahl index. Nowadays systemically important banks are those who are highly interconnected with others. To measure the importance of interconnections, an important distinction arises between ex ante and ex post metrics. Ex ante measures determine the contribution of each bank to systemic risk based on a time- t static configuration of the network. These measures are useful as they identify banks/nodes which can potentially be risk spreaders but they have little predictive power, as they do not consider the transformations in the network topology following shocks. On the contrary ex post measures do so, hence they can be fruitfully used in stress tests. Overall ex ante measures can be used for preemptive actions, while ex post measures can be used to predict the possible extent of contagion in the aftermath of shocks, an information crucial to establish the correct implementation of post-crisis remedies.

For brevity we decided to report the analytical description of the ex ante metrics and their performance in the numerical analysis in [Appendix D](#). In the main text we focus on one ex post metric, the Shapley value (see [Shapley \(1953\)](#), and [Bluhm et al. \(2013\)](#) and [Drehmann and Tarashev](#)

²⁷A schematic representation of the shock transmission process is given in [Figure 6](#) in [Appendix C](#).

(2011) for applications to banking), and we comment on the comparison with other ex ante metrics. The Shapley value, borrowed from the literature on cooperative and non-cooperative game theory, provides the contribution (through permutations) of each bank to an aggregate value. The latter in our case is the aggregate probability of default and is computed via the ratio of assets from all defaulting banks to total assets, $\Phi = \frac{\sum_{\Omega} assets_{\Omega}}{\sum_i assets_i}$, where $\Omega \in i$ identifies the set of defaulting banks (banks that cannot fulfill regulatory requirements even after selling all assets). One desirable property of the Shapley value is additivity, which in our case implies that the marginal contribution of each bank adds up to the aggregate default probability. The additivity property facilitates the implementability of macro-prudential instruments at individual bank levels since capital requirements can be designed as linear transformations of the marginal contribution.

Formally the Shapley value is defined as follows. Define $O : 1, \dots, n \rightarrow 1, \dots, n$ to be a permutation that assigns to each position k the player $O(k)$. Furthermore denote by $\pi(N)$ the set of all possible permutations with player set N . Given a permutation O , and denoting by $\Delta^i(O)$ the set of predecessors of player i in the order O , the Shapley value can be expressed in the following way:

$$\Xi_i(v^{\Psi}) = \frac{1}{N!} \sum_{O \in \pi_N} (v^{\Psi}(\Delta^i(O) \cup i) - v^{\Psi}(\Delta^i(O))) \quad (13)$$

where $v^{\Psi}(\Delta^i(O))$ is the value obtained in permutation O by the players preceding player i and $v^{\Psi}(\Delta^i(O) \cup i)$ is the value obtained in the same permutation when including player i . That is, $\Xi_i(v^{\Psi})$ gives the average marginal contribution of player i over all permutations of player set N . Note that the index Ψ denotes different possible shock scenarios, hence banks' contribution to systemic risk is computed conditional on a shock vector to the banking system.²⁸

4 Baseline Scenario Results and Empirical Matching

In this section we present the baseline network configuration, which we analyze under the three matching algorithms previously described. We characterize the baseline configuration of the network under each matching algorithm using synthetic metrics, namely density, average path length, assortativity, clustering, betweenness and eigenvector centrality. Our primary goal is to verify that our banking network shares topological properties with the empirical counterparts. We indeed find that our model is able to replicate a number of empirical properties (core-periphery, low density and dis-assortative behavior), particularly so under certain matching algorithms.

Before presenting the simulation results for the baseline structure, we describe the model cal-

²⁸Due to the curse of dimensionality, the Shapley value is normally approximated in numerical simulations by the average contribution of banks to systemic risk over k randomly sampled permutations, $\Xi_i(v^{\Psi}) \approx \hat{\Xi}_i(v^{\Psi}) = \frac{1}{k} \sum_{O \in \pi_k} (v^{\Psi}(\Delta^i(O) \cup i) - v^{\Psi}(\Delta^i(O)))$.

ibration, which is largely based on banking and regulatory data. [Table 1](#) summarizes calibrated values and shock distributions.

Following [Drehmann and Tarashev \(2011\)](#), the number of banks is set to 20. This allows to replicate a fairly concentrated structure. The liquidity requirement parameter, α , is set to 10%, mimicking the cash reserve ratio in the U.S. The equity ratio requirement is set to 8%, following Federal Reserve regulatory definitions and also in line with Basel III. The banks' capital buffer (on top of the equity requirement) is set to 1%. Risk weights are set according to regulatory policy: ω_n , the risk weight on non-liquid assets, is set equal to 1 in accordance with the weights applied in Basel II for commercial bank loans; ω_l , the risk weight on interbank lending, is set to 0.2, which is the actual risk weight used for interbank deposits in OECD countries. We use data from Bureau van Dijk's Bankscope database to calibrate deposits and equity. We take the average of total assets for the period 2011-2013 for Euro Area banks, and use deposits and equity (again averaged over 2011-2013) of the top 20 banks in terms of assets.²⁹ The return on non-liquid assets is randomly drawn from a uniform distribution over the range 0 – 15%,³⁰ whereas the vector of shocks to non-liquid assets, which is the starting point of the shock transmission process, is drawn from a multivariate normal distribution with a mean of 5, a variance of 25 and zero covariance (we draw 1000 shocks to evaluate the model). The variance is set high enough so as to capture the possibility of high stress scenarios. We set the loss given default parameter ξ to 0.5 (see for instance [Memmel and Sachs \(2013\)](#)), whereas for the expected probability of default and its variance we assign values of 0.5% and 0.3% respectively. Finally, the banks' risk aversion parameter σ is set equal to 2. For precautionary saving to arise such parameter must be larger than 1.

We start by describing the partitions of banks into borrowers and lenders and the equilibrium interbank rate. Notice that those features hold independently from the trading algorithm since banks' optimization and price tâtonnement are the same for every matching of traded quantities. Given the above calibration, the equilibrium interbank rate is 2.98%, in line with the pre-crisis average of EONIA. There are 5 banks that only lend (banks 6, 10, 16, 17 and 19), 6 that only borrow (2, 5, 7, 8, 14 and 15) and 9 that both borrow and lend (1, 3, 4, 9, 11, 12, 13, 18 and 20). Generally speaking banks who borrow are those whose returns on non-liquid assets are high. Since those have good investment opportunities they wish to invest and require liquidity beyond the one present in their portfolio. On the contrary banks decide to lend when the rate that they receive on bank lending is higher than the rate of return on non-liquid assets. The convexity of the optimization problem implies that internal solutions exist and banks can be on both sides of the market, namely being borrowers and lenders at the same time. Few large banks enter both sides of the market and act as central nodes: those banks have high returns on non-liquid assets, hence they wish to obtain

²⁹The banks used for calibration are Deutsche Bank, BNP Paribas, Crédit Agricole, Société Générale, Santander, ING, UniCredit, Intesa Sanpaolo, Commerzbank, BBVA, Natixis, Caixabank, KBC, CIC, Banca Monte dei Paschi di Siena, Erste Group Bank, Deutsche Postbank, Banco Popular Español, Bank of Ireland, and Banco de Sabadell.

³⁰The variance is computed accordingly.

Par./Var.	Description	Value
N	Number of banks in the system	20
α	Liquidity requirement ratio	0.10
ω_n	Risk weight on non-liquid assets	1
ω_l	Risk weight on interbank lending	0.20
γ	Equity requirement ratio	0.08
τ	Desired equity buffer	0.01
d_i	Bank deposits	Top20 EA
e_i	Bank equity	Top20 EA
σ	Bank risk aversion	2
ξ	Loss given default	0.5
$E[pd]$	Expected default probability	0.005
σ_{pd}^2	Variance of default probability	0.003
r_i^n	Return on non-liquid assets	$U(0, 0.15)$
$\sigma_{r_i^n}^2$	Variance of r_i^n	$\frac{1}{12}(\max(r_i^n) - \min(r_i^n))^2$
Ψ	Shocks to non-liquid assets	$\mathcal{N}(\mathbf{5}, 25 * \mathbf{I})$

Table 1: Baseline calibration

liquidity for investment, but they also have large cash balances and are willing to lend to acquire a diversified portfolio.

4.1 Synthetic Measures of Network Architecture and Empirical Matching

Our next step is to describe the network topology under the three alternative matching algorithms and by using synthetic network indicators, which are density, average degree, average path length, betweenness, eigenvector centrality, clustering and assortativity.³¹ Notice that synthetic metrics describing the network largely depend upon the banks' optimization problem and upon the matching algorithms. On the other hand, for the static network configuration the three contagion channels described previously do not play a role since they become operative only when banks are hit by shocks. The network response to shocks and the role of the contagion channels for systemic risk will be analysed in Section 5.

Figure 1 presents the interbank network obtained through the RAS method (maximum entropy algorithm), given the parameters from Table 1. Different nodes represent banks and their size is given by total assets. The width of arrows indicates the amounts transacted and an arrow going from i to j indicates that i is exposed to j through lending. The network has a classical configuration

³¹To compute some of the network indicators we made use of the [Brain Connectivity Toolbox](#) and the [MatlabBGL](#) library.

of evenly sparse links with few central nodes that provide most of the liquidity in the system. The density of this network is 52.9% (see [Table 2](#) below), which is higher than the one usually observed in country-specific studies on interbank networks, but is nonetheless in line with the density of the total exposure network of large European banks (60%) presented in [Alves et al. \(2013\)](#).

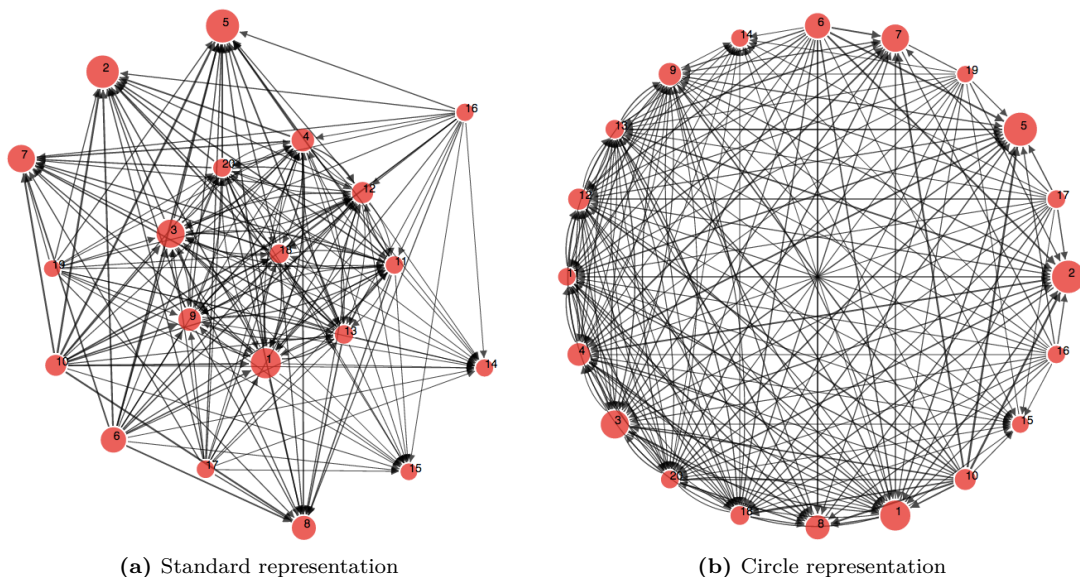


Figure 1: Baseline network with Maximum Entropy (RAS)

[Figure 2](#) presents the baseline configuration with an interbank matrix computed via the closest matching algorithm. In this case there are notably less links, and given that the same amount is transacted in the market, we also see an increase in the width of the arrows. The density of the network is now 7.37%, which is more in line with the evidence from country-specific studies of interbank markets (see for instance [van Lelyveld and In't Veld \(2012\)](#) for the Dutch case). Recall that the closest matching algorithm produces the lowest density among the three algorithms considered.

Finally, [Figure 3](#) shows the interbank matrix obtained via the random matching algorithm. We set the loading parameter $\lambda = 0.99$ and this translates into a density of 22.37%, a number which is in between the ones obtained with the other two algorithms.³² This network features more links and with wider arrows than the previous one.

In terms of density properties the network which more resembles empirical counterparts is the one obtained through closest matching. This is also the algorithm advocated by [Shubik \(1999\)](#) as most apt to capture clearing in borrowing and lending relations.

³²This density is more in line with that presented in [Fricke and Lux \(2012\)](#) for Italian banks in the e-mid trading platform.

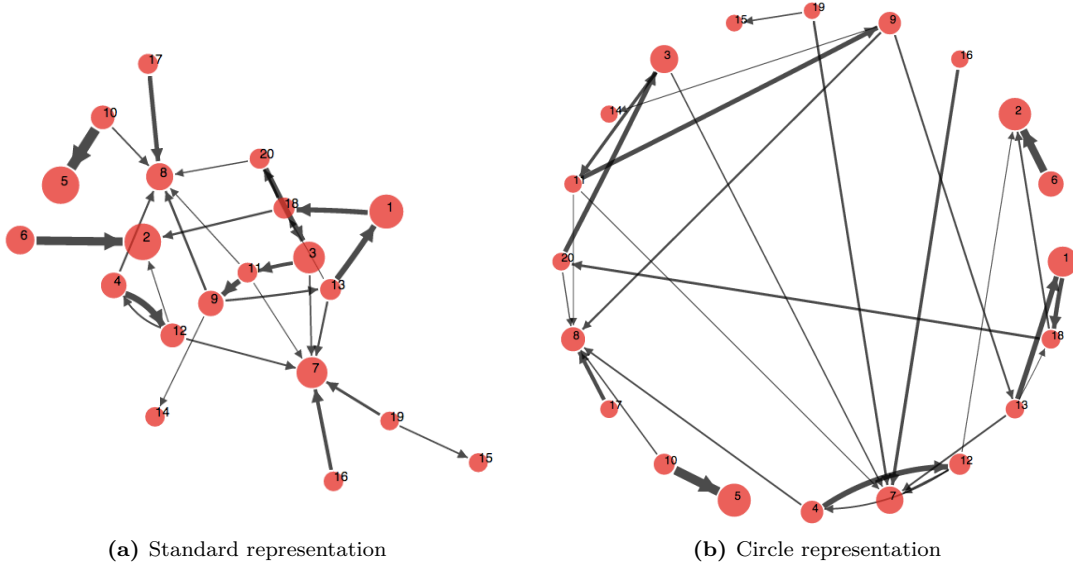


Figure 2: Baseline network with Closest Matching (CMA)

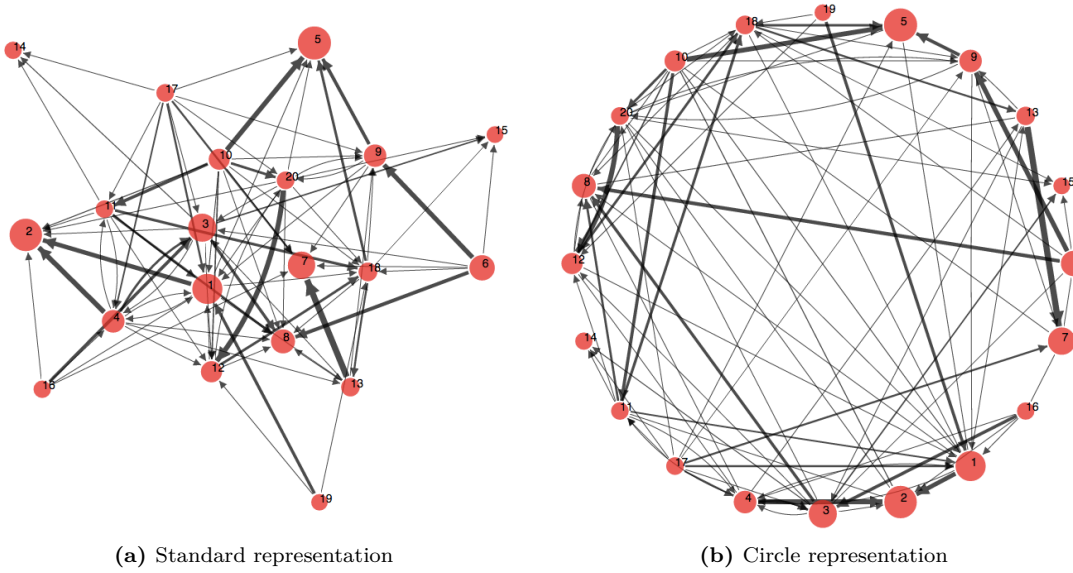


Figure 3: Baseline network with Random Matching (RMA)

Table 2 shows results for the other synthetic metrics considered under all three matching algorithms and given the baseline parameterization.

	RAS	CMA	RMA
Density (%)	52.89	7.37	22.37
Degree (Av.)	10.05	1.40	4.25
Av. Path Length	1.08	2.60	1.51
Betweenness Cent. (Av.)	1.00	7.10	23.75
Eigenvector Cent.(Av.)	0.17	0.13	0.08
Clustering Coeff. (Av.)	0.27	0.03	0.14
Assortativity			
<i>out-in degree</i>	-0.50	-0.15	-0.10
<i>in-out degree</i>	-0.03	0.26	-0.13
<i>out-out degree</i>	-0.29	-0.31	-0.31
<i>in-in degree</i>	-0.26	-0.44	-0.27

Table 2: Network characteristics - Baseline setting

The first two network metrics are closely related. The density of the network captures the share of existing links over the total amount of possible links, whereas the average degree gives the average number of connections per bank. Both metrics proxy the extent of diversification in the network. By construction, in the RAS network both density and average number of connections per bank are higher, while the opposite holds for the CMA network, with the RMA lying in between.

The average path length is the mean shortest path between pairs of nodes. In the RAS network any given bank is essentially one step away; for the RMA this number goes roughly to 1.5, whereas in the CMA network is 2.6, implying that the average bank is almost 3 connections away. Overall, the average path length is small, in line with real-world interbank networks (see [Alves et al. \(2013\)](#) or [Boss et al. \(2004\)](#) among others). This implies that exposure is not far away for the average bank in the network.

Betweenness and eigenvector centrality are computed as averages for all nodes in the network. Betweenness score is low for the RMA network, but this is due primarily to the random nature of the trading partner assignment. On the other side the CMA configuration features high betweenness and eigenvector centrality since in this case a few banks act as gatekeepers.

The clustering coefficient measures the tendency of neighbors of a given node to connect to each other, thereby generating a cluster of connections. The average clustering coefficient is, not surprisingly, relatively high for the RAS network, and is reduced notably for the CMA network, with the RMA network being in between. Even the value for the RAS network is low relative to other types of networks and in line with evidence on real-world interbank networks.

The assortativity coefficient aims at capturing the tendency of high-degree nodes to be linked to other high-degree nodes. As noted by [Bargigli et al. \(2013\)](#), interbank networks tend to be dis-assortative, implying that high-degree nodes tend to connect to other high-degree nodes less

frequently than would be expected under the assumption of a random rewiring of the network that preserves the nodes' degrees. All the networks we consider show in fact dis-assortative behavior for all assortativity measures, the exception being the CMA network which has positive in-out degree assortativity. These results are in line with those observed in the data (see for instance [Bech and Atalay \(2008\)](#), [Bargigli et al. \(2013\)](#) or [Alves et al. \(2013\)](#)). Notice that dis-assortative behavior is associated with core-periphery structures; this is true both in the data and in our model (this is also visible by our graphs).

To sum up our network shares most synthetic indicators with the empirical counterparts. Notably the network is characterized by low density, low clustering and dis-assortative behavior (core-periphery structure). Further results for the simulation of the baseline network can be found in [Appendix E](#).

5 Model Response to Shocks: Systemic Risk and Systemic Importance

An essential prerequisite of prudential regulation consists in measuring systemic risk and identifying systemically important banks. Assessing indeed the contribution of each bank to risk propagation is a crucial aspect of the inspecting activity that supervisors conduct to prevent crises. To this aim and prior to the analysis of the prudential policy we present some metrics that measure the contribution of each bank to systemic risk or that allow the supervisor to detect systemically important intermediaries. In this section we focus specifically on the Shapley value. Given the system-wide default probability following a multinomial distribution of banks' shocks, the Shapley value determines the contribution of each bank to it. Other centrality metrics are used to identify systemically important banks. At the end of the section we comment on the comparison between the ranking of systemically important banks obtained through those alternative metrics and the one obtained through the Shapley value. Numerical results for the alternative metrics are presented in [Appendix E](#).

[Figure 4](#) presents each bank's contribution to systemic risk, based on the Shapley Value methodology. The number of permutations considered for the computation of the Shapley Value was set to 1000. The clearing algorithm used is that of [Eisenberg and Noe \(2001\)](#). We simulate shocks to the value of non-liquid assets with multinomial distributions. In response to those shocks all channels of contagion are activated. Losses in asset values indeed might force some banks to renege on their interbank debt obligations, thereby producing interconnection risk cascades. Asset losses also imply that some banks are unable to meet regulatory constraints, thereby engaging in asset sales. In face of uncertainty liquidity hoarding increases the inability of banks to repay interbank debt, thereby increasing the scope for loss cascades.

Our focus for this simulation is on two dimensions. First, we are interested in the relation between the network topological properties and systemic risk. The former are usually the result of institutional features and depend upon the overall financial architecture. It is important to single out which of those topological properties help in improving financial stability. Second, we are interested in understanding which economic channels explain why some banks contribute to risk more than others.

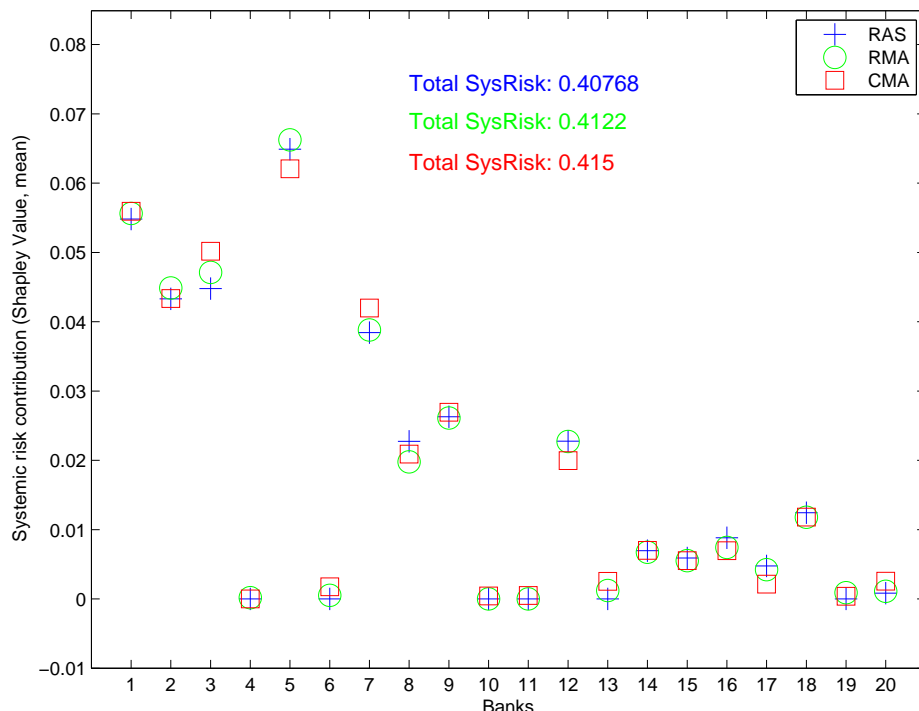


Figure 4: Contribution to systemic risk (mean Shapley Value), by bank and by network

On the first aspect, namely the relation between risk and network topology, the following considerations are in order. First, for all three matching algorithms, there is no strong relationship between density and systemic risk. However we see that the lower connectivity network, namely the CMA, presents the highest systemic risk, whereas the highest connectivity network, namely the RAS, features the lowest degree of systemic risk, with the RMA network scoring in between the two³³.

Regarding the second goal, namely assessing the role of each bank in contributing to systemic risk, the following considerations are in order. By jointly analyzing the data in Figure 4 and the

³³While the numbers look similar, it should be noted that these numbers are obtained as averages across 1000 realizations of shocks. For any given realization of the shock vector it need not be the case that the contribution of any given bank is similar for the three different networks.

banks' optimal portfolio allocations as reported in [Table 4](#) in [Appendix E](#) we find that the banks which contribute the most to systemic risk are the ones which both borrow in the interbank market and invest highly in non-liquid assets.³⁴ Generally speaking we find a strong connection between Shapley value and total assets. Interbank borrowing increases the extent of risk transmission through direct interconnections, while investment in non-liquid assets increases the extent of risk transmission via fire sale externalities. The more banks borrow and the more banks invest in non-liquid assets, the larger is their contribution to systemic risk. The rationale behind this is as follows. Banks which leverage more in the interbank market are clearly more exposed to the risk of default on interbank debts. The larger is the size of debt default the larger are the losses that banks transmit to their counterparts. Borrowing banks therefore contribute to systemic risk since they are the vehicle of network/interconnection externalities. On the other hand, banks which invest more in non-liquid assets transmit risks since they are the vehicle of the pecuniary externalities. The higher is the fraction of non-liquid asset investment, the higher is the negative impact that banks' fire sales have on market prices. The higher is the collapse in market prices, the higher are the accounting losses experienced by all other banks due to asset commonality and mark-to-market accounting. Notice that banks which invest and borrow much are also those with the highest returns on non-liquid assets investment. As banks invest more they also grow in size, hence we also see a connection between banks' size and systemic risk. [Figure 4](#) (observed in combination with total assets as from [Table 4](#) which presents the optimal balance sheet structure in the baseline setting) shows for instance that smaller banks tend to contribute less to systemic risk. While the Shapley value shows a strong connection to total assets, the connection to other balance sheet items or relevant balance sheet ratios, regardless of the network considered, is not particularly strong (see [Figure 7](#) in [Appendix E.2](#)). To assess the role of banks' risk aversion and precautionary savings on the transmission of risk we present the main results for systemic risk by comparing the models with and without risk averse banks: see [Appendix F](#). Generally speaking systemic risk is higher with risk averse banks. In the face of uncertainty banks' marginal utility from hoarding liquidity increases. The fall in interbank supply drives interbank rates up, which in turn increases debt default rates. Second, introducing convex preferences generally increases the degree of non-linearity featured by the model.

To test the robustness of the Shapley value we compute the ranking of systemically important banks also using alternative metrics. Simulation results for those are presented in [Appendix E.2](#). [Figure 8](#) shows that also for other metrics a positive connection exists between systemic importance and total assets. [Table 5](#) presents the ranking of banks' systemic importance under the three alternative matching algorithms according to the network centrality metric. [Table 6](#) presents the same but for input-output measures of systemic importance. The ranking of banks is on average confirmed under alternative metrics and across different matching algorithms. The only noteworthy

³⁴Usually those are also the banks with the higher returns on non-liquid assets investment.

characteristic is that the metrics of network centrality present more variations than other metrics. One may also wonder whether rankings based on systemic importance deliver similar results as those based on systemic risk indicators (say, input-output measures versus Shapley value). [Figure 8](#) in [Appendix E.2](#) provides some evidence that in fact this is not the case.

6 Policy Analysis

Recent guidelines on prudential regulation from Basel III include requirement ratios both for equity and for liquidity. A crucial policy question is whether changing the regulatory requirements affects systemic risk and the contribution of each bank to it. We therefore inspect the variations in systemic risk and the optimal allocation for different values of the liquidity requirement α and of the equity requirement γ . As in the baseline setting, the number of permutations for the computation of the Shapley Value is set to 1000.

[Table 3](#) summarizes the main results from the policy experiments. To the left (right) we have the results from changes in the liquidity (equity) requirement. The upper panel presents total systemic risk for the three networks considered, the middle panel presents interbank assets as a share of total assets and the lower panel presents non-liquid assets as a share of equity.

We start by examining how overall systemic risk and the contribution of each bank to it change when altering the two policy parameters. At first glance, overall systemic risk shows a downward trend when we increase the liquidity parameter α . That said, as is obvious from the charts, starting from values around 0.2 systemic risk exhibits a jig-saw behaviour within this general downward trend. Such behaviour is not present in the linear model without uncertainty and we therefore attribute it to the non-linearities embedded in the set-up of our model. Regardless of the network configuration, and for all values of α considered, there are some banks that always contribute to systemic risk (mostly banks 1, 2, 3, 5, 12 and 16, see [Figure 15](#), [Figure 17](#) and [Figure 19](#)). Note that the bank-specific charts as well as the overall systemic risk plot present confidence bands from the 1000 shock realizations. The rationale for the results is as follows. As banks must hold more liquidity for precautionary motives, their exposure in the interbank market declines, though this is not reflected in interbank assets as a share of total assets since the reduction in non-liquid assets is quite substantial (see the lower left panel in [Table 3](#)). The interbank interest rate increases due to the scarce supply of liquidity (see middle-left panel in [Table 8](#) in [Appendix G](#)) and banks' investment in non-liquid assets declines as available liquidity falls. Overall, there is a strong reduction in the scope for fire sale externalities and a relatively milder increase in the scope for network externalities. The ratio of non-liquid assets to equity is halved for the range of values of α under consideration, pointing to the trade off between stability (as proxied by risk) and efficiency (as proxied by aggregate investment in non-liquid assets).

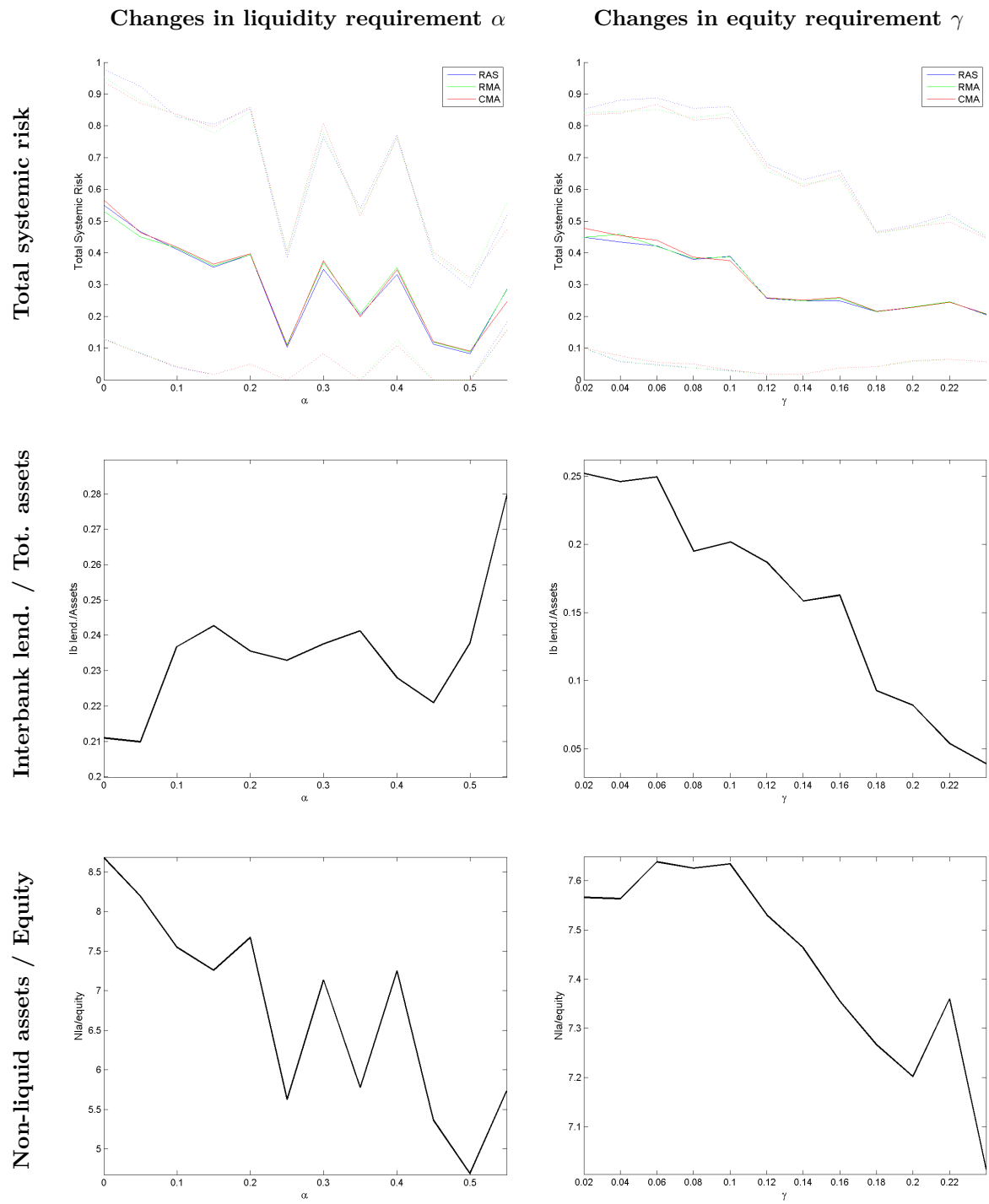


Table 3: Main results from policy analysis

Results are somehow more complex when we increase the equity requirement, γ .³⁵ As this parameter increases, overall systemic risk declines over an initial range but it stays flat after roughly 0.13. Banks leverage less and the interbank interest rate declines as the demand of liquid funds has declined (see upper and mid-right panels in [Table 8](#) in [Appendix G](#)). This reduces the overall scope for transmitting default losses, and in fact interbank lending as a percentage of assets reaches very low values (see middle right panel in [Table 3](#)). However, banks also reduce the amount of liquid assets (not shown here), while keeping the amount of non-liquid asset investment roughly unchanged in terms of equity for an initial range and then only reducing it slightly (see [Table 3](#) and compare the y-axis of the middle right and middle left panels). The scope of risk transmission through fire sales is therefore only slightly reduced. Increasing the equity requirement above 10% seems to have a non-negligible impact on systemic risk, while at the same time not reducing efficiency as strongly as with increases in the liquidity requirement. As for the contribution of each bank to overall systemic risk (see Shapley values in [Figure 16](#), [Figure 18](#), [Figure 20](#)) we observe that, while most banks tend to transmit less risk as γ increases, others instead tend to contribute more. Since all banks are less exposed to the interbank market the scope of loss cascades through network linkages is reduced. On the other hand some banks invest more in non-liquid assets. This exposes the latter to the swings in the market price for non-liquid assets and increases the probability that they will engage in fire sales. The pattern described is pretty much common to all three network configurations considered.

We also examine some additional metrics (charts can be found in [Appendix G](#)). The lower panel of [Table 8](#) presents the evolution of network densities for the three networks and for the two policy experiments we entertain³⁶. For changes in the liquidity requirement, densities for each network stay within a narrow range with the exception of the RAS network which shows an increasing trend. The RMA stays within 20-25% and the CMA stays around 6-8%. On the other hand, when evaluating the model in response to changes in the equity requirement we see a notable decrease in density when γ goes above 0.12, and it stays low thereafter. The reason for this can be seen in [Figure 13b](#). The number of active banks in the interbank market drops substantially, in particular those banks that both borrow and lend. If we take the number of banks on both sides of the market as a proxy for intermediation activity, [Figure 13b](#) shows that intermediation reaches a peak when $\gamma = 0.12$. As the equity requirement increases less banks are active in the market and the ones that are actually active demand less liquidity relative to existing supply, forcing the continuous downward trend in the interbank rate that we see in [Table 8](#).

As [Figure 13a](#) shows, no such development occurs when increasing the liquidity requirement.

³⁵A subtle feature of both policy experiments that is worth mentioning is that mean systemic risk is not always higher for any given network: in fact we see the lines crossing each other several times, indicating that depending on the range of values for the policy parameters different networks deliver the highest systemic risk in expectation.

³⁶Average degree, path length and clustering coefficients paint a very similar picture so we left them out for the sake of space.

This essentially leaves the number of active banks unchanged. When the liquidity requirement increases there seem to be two countervailing forces that balance each other. As the liquidity requirement raises, banks supply less liquidity in the interbank market and this has a depressing effect on density and other measures such as closeness (not shown here). On the other hand, some banks increase their demand of liquid funds driving the interbank rate up and inducing other banks to substitute investment in non-liquid assets with interbank lending. This asset substitution effect increases the available liquidity in the interbank market (as shown in [Table 3](#)), which in turn has a positive impact on density and related measures.

To assess the contribution of each of the channels considered (interconnections, fire sales and liquidity hoarding) we compare the evolution of systemic risk (under different values for α and γ) under four alternative models (see [Appendix F](#)). *Model 1* is the benchmark considered so far. *Model 2* considers risk neutral banks with a linear objective function, thereby eliminating the liquidity hoarding channel and eliminating the possibility that banks act on both sides of the market. *Model 3* eliminates investment in non-liquid assets in order to shut off the fire sale channel. Finally, *Model 4* is a small variation on *Model 3* in which the risk aversion parameter σ is set to zero. The patterns of systemic risk so far described remain roughly unchanged with two noteworthy features. First, the benchmark model shows larger swings in the changes of systemic risk with respect to α and γ . This is due to the fact that the presence of risk averse agents by triggering precautionary saving features higher non-linearities. Second, in *Model 4* systemic risk increases with respect to increases in α . While this seems puzzling, it is well explained by absence of alternative investment opportunities as those in non-liquid assets, in combination with having $\sigma = 0$. As the liquidity requirement increases, banks which are short of funds increase their demand of interbank borrowing. This raises the interbank rate and renders interbank lending attractive for banks which have excess liquidity. Overall network linkages in the interbank market increase and so does contagion of default risk.

To sum up, increasing the liquidity requirement unequivocally reduces systemic risk as it reduces both the extent of network links and the investment in non-liquid assets. As a consequence an increase in α reduces the scope of both network and pecuniary externalities rendering the network more stable. The fall in the overall non-liquid asset investment shows however that an increase in the liquidity requirement reduces system efficiency. An increase in the equity requirement also decreases systemic risk (though the latter remains flat after $\gamma = 0.13$), but without a substantial decrease in efficiency.

7 Concluding Remarks

We have analyzed a banking network model featuring risk transmission via different channels. Banks in our model are risk averse and solve a concave optimal portfolio problem. The individual optimization problems and the market clearing processes deliver a matrix of network links in the

interbank market. Each bank can be both borrower and lender vis-à-vis different counterparties. Shocks to one bank are transmitted through defaults on interbank debt, through price collapses of non-liquid assets triggered by fire sales or through liquidity hoarding. Clearing in the market takes place through a price tâtonnement iterative process and through a trading matching algorithm. We considered three alternative trading matching algorithms, namely maximum entropy, closest matching (or minimum distance) and random matching. Each one of them produces a different architecture for the banking network in terms of density, average degree, average path length, assortativity, clustering, betweenness and eigenvector centrality. This also implies that risk transmits differently in each of the three network configurations.

We use our banking network to assess the role of prudential regulations in reducing systemic risk. We find that increasing the liquidity requirement unequivocally reduces systemic risk and the contribution of each bank to it. As banks must hold more liquidity for precautionary motives, their exposure in the interbank market declines, though this is not reflected in interbank assets as a share of total assets as the reduction in non-liquid assets is quite substantial. The former limits somewhat the scope for network externalities, whereas the latter substantially reduces the scope for pecuniary externalities. The reduction in non-liquid assets is so strong that there is an associated cost to it in terms of efficiency of the system, highlighting the existing trade-off between stability and efficiency. An increase in the equity requirements instead does not present this strong trade-off. Systemic risk decreases, in particular for an initial range of values of γ . The scope for network externalities is persistently reduced as the share of interbank assets over total assets steadily declines to reach very low values in the upper range of γ . While there is also a slight reduction in the scope for fire sales externalities, the reduction in non-liquid assets is relatively minor. Furthermore, evaluation based on input-output measures reveals that the system becomes more homogenous and the potential damage from interbank market collapses is markedly reduced. This comes at the expense of having less banks trade in the interbank market, with an associated reduction in its density.

References

- Afonso, G. and Shin, H. S. (2011). Precautionary demand and liquidity in payment systems. *Journal of Money, Credit and Banking*, 43:589–619.
- Aldasoro, I. and Angeloni, I. (2014). Input-output-based measures of systemic importance. *Quantitative Finance*, (<http://dx.doi.org/10.1080/14697688.2014.968194>).
- Allen, F. and Gale, D. (2000). Financial contagion. *Journal of Political Economy*, 108(1):1–33.
- Alves, I., Ferrari, S., Franchini, P., Heam, J.-C., Jurca, P., Langfield, S., Laviola, S., Liedorp, F., Sánchez, A., Tavoraro, S., and Vuilleme, G. (2013). Structure and resilience of the european interbank market. Occasional Papers 3, European Systemic Risk Board.
- Bargigli, L., di Iasio, G., Infante, L., Lillo, F., and Pierobon, F. (2013). The multiplex structure of interbank networks. Technical report, arXiv.org.
- Battiston, S., Delli Gatti, D., Gallegati, M., Greenwald, B., and Stiglitz, J. E. (2012). Liaisons dangereuses: Increasing connectivity, risk sharing, and systemic risk. *Journal of Economic Dynamics and Control*, 36(36):1121–1141.
- Bech, M. L. and Atalay, E. (2008). The topology of the federal funds market. Staff Reports 354, Federal Reserve Bank of New York.
- Bluhm, M., Faia, E., and Krahnen, J. P. (2013). Endogenous banks’ networks, cascades and systemic risk. Unpublished Manuscript.
- Boss, M., Elsinger, H., Summer, M., and Thurner, S. (2004). Network topology of the interbank market. *Quantitative Finance*, 4:677–684.
- Caballero, R. J. and Simsek, A. (2013). Fire sales in a model of complexity. *Journal of Finance*, 68(6):2549–2587.
- Caccioli, F., Farmer, J. D., Foti, N., and Rockmore, D. (2014). Overlapping portfolios, contagion, and financial stability. *Journal of Economic Dynamics and Control*, (<http://dx.doi.org/10.1016/j.jedc.2014.09.041>).
- Cifuentes, R., Ferrucci, G., and Shin, H. S. (2005). Liquidity risk and contagion. *Journal of the European Economic Association*, 3(2-3):556–566.
- Diamond, D. W. and Dybvig, P. H. (1983). Bank runs, deposit insurance, and liquidity. *Journal of Political Economy*, 91(3):401–19.
- Drehmann, M. and Tarashev, N. (2011). Measuring the systemic importance of interconnected banks. BIS Working Paper 342, Bank for International Settlements.

- Duffie, D. and Zhu, H. (2011). Does a central clearing counterparty reduce counterparty risk? *Review of Asset Pricing Studies*, 1(1):74–95.
- Eisenberg, L. and Noe, T. H. (2001). Systemic risk in financial networks. *Management Science*, 47(2):236–249.
- Elliott, M. L., Golub, B., and Jackson, M. O. (2014). Financial networks and contagion. *American Economic Review*, 104(10):3115–53.
- Fricke, D. and Lux, T. (2012). Core-periphery structure in the overnight money market: Evidence from the e-mid trading platform. Kiel Working Papers 1759, Kiel Institute for the World Economy.
- Gai, P., Haldane, A., and Kapadia, S. (2011). Complexity, concentration and contagio. *Journal of Monetary Economics*, 58(5).
- Gale, D. and Shapley, L. (1962). College admissions and the stability of marriage. *American Mathematical Monthly*, 69:9–15.
- Glasserman, P. and Young, P. (2014). How likely is contagion in financial networks? *Journal of Banking & Finance*, (<http://dx.doi.org/10.1016/j.jbankfin.2014.02.006>).
- Greenwald, B. and Stiglitz, J. E. (1986). Externalities in economies with imperfect information and incomplete markets. *The Quarterly Journal of Economics*, 101(2):229–264.
- Greenwald, B. C. and Stiglitz, J. E. (1993). Financial market imperfections and business cycles. *The Quarterly Journal of Economics*, 108(1):77–114.
- Gul, F. (1989). Bargaining foundations of shapley value. *Econometrica*, 57(1):81–95.
- Halaj, G. and Kok, C. (2014). Modeling emergence of the interbank networks. Working Paper 1646, European Central Bank.
- Langfield, S. and Soramäki, K. (2014). Interbank exposure networks. *Computational Economics*, (forthcoming).
- Mas-Colell, A., Whinston, M. D., and Green, J. R. (1995). *Microeconomic Theory*. Oxford University Press.
- Mommel, C. and Sachs, A. (2013). Contagion in the interbank market and its determinants. *Journal of Financial Stability*, 9(1):46–54.
- Shapley, L. (1953). A value for n-person games. In Kuhn, H. and Tucker, A., editors, *Contributions to the Theory of Games*, volume II of *Annals of Mathematical Studies*, pages 307–317. Princeton University Press.
- Shapley, L. S. and Shubik, M. (1972). The assignment game i: The core. *International Journal of Game Theory*, 1:111–130.
- Shubik, M. (1999). *The Theory of Money and Financial Institutions*, volume Volume 1. The MIT Press.

- Upper, C. (2011). Simulation methods to assess the danger of contagion in interbank markets. *Journal of Financial Stability*, 7(3):111–125.
- van Lelyveld, I. and In't Veld, D. (2012). Finding the core: Network structure in interbank markets. DNB Working Papers 348, Netherlands Central Bank.

A Second Order Approximation of the Utility Function

The generic utility of profits is given by

$$U(\pi) \tag{14}$$

The second order approximation of the utility Equation 14, in the neighborhood of the expected value of profits $E[\pi]$ reads as follows³⁷:

$$U(\pi_i) \approx U(E[\pi_i]) + U_\pi(\pi_i - E[\pi_i]) + \frac{1}{2}U_{\pi\pi}(\pi_i - E[\pi_i])^2 \tag{15}$$

Taking expectations on both sides of equation 15 yields:

$$\begin{aligned} E[U(\pi_i)] &\approx \underbrace{E[U(E[\pi_i])]}_{=U(E[\pi_i]) \text{ by LIE}} + U_\pi \underbrace{E[(\pi_i - E[\pi_i])]}_{=0 \text{ by LIE}} + \frac{1}{2}U_{\pi\pi} \underbrace{E[(\pi_i - E[\pi_i])^2]}_{=\text{Var}(\pi_i)=\sigma_\pi^2} \\ &\approx U(E[\pi_i]) + \frac{1}{2}U_{\pi\pi}\sigma_\pi^2 \end{aligned} \tag{16}$$

Given the CRRA function $U(\pi_i) = \frac{(\pi_i)^{1-\sigma}}{1-\sigma}$, where σ is the coefficient of risk aversion, we can compute the second derivative as $U_{\pi\pi} = -\sigma E[\pi_i]^{-(1+\sigma)}$. Notice that under certainty equivalence (namely when $E[U'''(\pi)] = 0$) the equality $E[U(\pi_i)] = U(E[\pi_i])$ holds at all states. With CRRA utility, the third derivative with respect to profits is positive, which in turn implies that the expected marginal utility grows with the variability of profits. Furthermore since, $U'' < 0$, expected utility is equal to the utility of expected profits minus a term that depends on the volatility of bank profits and the risk aversion parameter. This is a direct consequence of Jensen's inequality and provides the standard rationale for precautionary saving. Using the expression derived above for $U_{\pi\pi}$, the expected utility of profits can be written as:

$$E[U(\pi_i)] \approx \frac{E[\pi_i]^{1-\sigma}}{1-\sigma} - \frac{\sigma}{2}E[\pi_i]^{-(1+\sigma)}\sigma_\pi^2 \tag{17}$$

Next we derive an expression for the variance of profits. Notice that volatility only derives from uncertainty in non-liquid asset returns and from default premia on borrowing. Given the source of uncertainty we obtain the following volatility of profits:

$$\sigma_\pi^2 = \text{Var}\left(r_i^n n_i + r^l l_i - \frac{1}{1-\xi p d_i} r^l b_i\right) = n_i^2 \sigma_{r_i^n}^2 - (b_i r^l)^2 \text{Var}\left(\frac{1}{1-\xi p d_i}\right) + 2n_i r^l b_i \text{cov}\left(r_i^n, \frac{1}{1-\xi p d_i}\right) \tag{18}$$

We know that $p d_i \in [0, 1]$. Furthermore, even when $f(p d_i) = \frac{1}{1-\xi p d_i}$ is a convex function, over

³⁷Note that all partial derivatives are also evaluated at $E[\pi]$.

a realistic range of pd_i it is essentially linear and it is therefore sensible to obtain the variance of $f(pd_i)$ through a first order Taylor approximation around the expected value of pd_i , which yields:

$$\text{Var} \left(\frac{1}{1 - \xi pd_i} \right) = \xi^2 (1 - \xi E[pd_i])^{-4} \sigma_{pd_i}^2 \quad (19)$$

We assume that the ex ante correlation between return on non-liquid assets and costs of borrowing is zero, hence we can set the covariance term in Equation 18 to zero. This leaves us with the following objective function:

$$E[U(\pi)] \approx \frac{E[\pi]^{1-\sigma}}{1-\sigma} - \frac{\sigma}{2} E[\pi]^{-(1+\sigma)} \left(n_i^2 \sigma_{r_i}^2 - (b_i r^l)^2 \xi^2 (1 - \xi E[pd_i])^{-4} \sigma_{pd_i}^2 \right) \quad (20)$$

B Model's Visual Representation

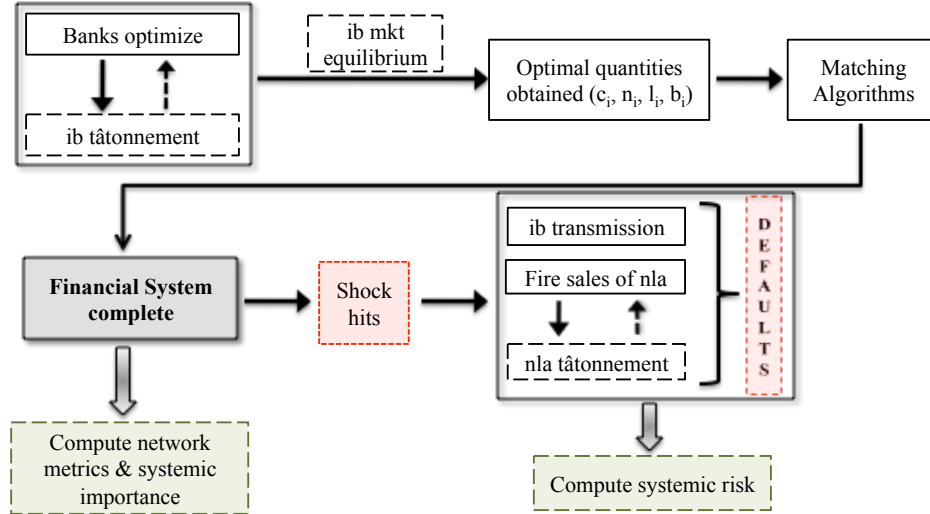


Figure 5: A bird's eye view of the model.

C Shock Transmission

A schematic representation of the shock transmission process is given in Figure 6. As noted earlier, after the vector of shocks is drawn the supply of non-liquid assets will be affected and therefore the price will have to be adjusted. Following such adjustment, some banks may not be able to fulfill their interbank commitments. Such banks will liquidate their entire non-liquid asset holdings, pay

as much as they can to interbank creditors and be added to the default set³⁸. At the same time, many banks may not be able to fulfill the equity requirement. Within this group, two sub-groups may be distinguished. First there are those banks that after selling part of their non-liquid asset holdings will be able to fulfill the equity requirement; the second group cannot fulfill the requirement even after selling all their non-liquid assets. The former group will just liquidate what it needs in order to comply with requirements, whereas the latter group will liquidate all and be added to the default set. All the non-liquid assets put on the market by all banks will be used for a recalculation of the price p and start a new round of the transmission process. When no more defaults occur the algorithm stops and systemic risk is computed as set out in the main text.

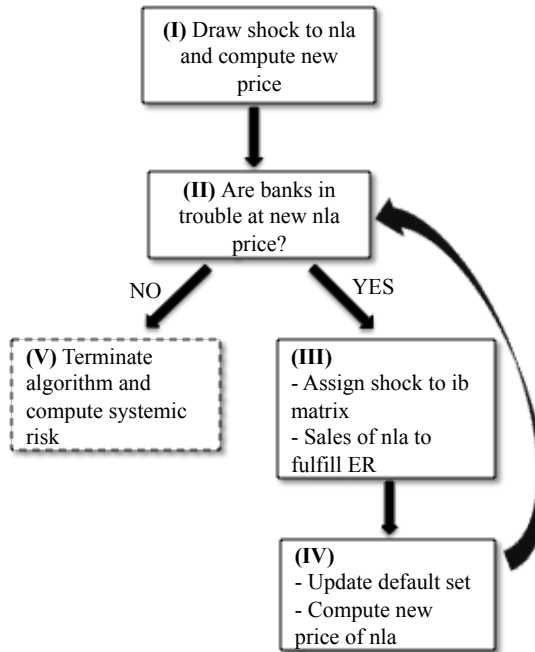


Figure 6: A stylized representation of the shock transmission process.

D Systemic Importance

We make use of two types of systemic importance measures. At first we consider centrality measures, which are somehow the most immediate evolution of traditional concentration indices. In graph theory and network analysis the centrality of a vertex or node measures its relative importance

³⁸The interbank adjustment is done following the now classic algorithm outlined in Eisenberg and Noe (2001). Note that, at this stage, interbank connections are taken as given and banks are not re-optimizing; changes to the interbank market structure are at this point the result of applying the clearing mechanism of Eisenberg and Noe (2001).

within the graph. In particular, we consider the following measures: degree, closeness, betweenness and eigenvector centrality³⁹.

Let the network be represented by an adjacency matrix \mathbf{G} , where an element $g_{ij} \neq 0$ indicates the existence of a connection between banks i and j . Degree centrality, which capture the immediate risk of receiving losses, shall be adapted in our model to take into account in- and out-degree: the former indicating the number of connections “arriving” to a node, the latter the number of connections “leaving” a node. In matrix notation they can be easily represented as $\mathbf{c}'_{(in)} = \mathbf{i}'\mathbf{G}$ and $\mathbf{c}_{(out)} = \mathbf{G}\mathbf{i}$, where \mathbf{i} is a column unit vector of appropriate dimension and a prime indicates the transposed of a vector. A generalization of degree-type measures is eigenvector centrality, which is given by the eigenvector corresponding to the largest eigenvalue of the matrix defining the network. Intuitively links to nodes with high centrality score should carry more weight than links to low-scoring nodes, and this is precisely the logic behind eigenvector centrality.

Closeness centrality captures the importance of distance among nodes. A bank is important to the extent that it is “close” to other banks, hence more likely to transmit distress. For node i , closeness centrality measures the shortest path between i and all other nodes reachable from it, averaged across all other nodes⁴⁰.

Finally, betweenness centrality assigns a high centrality score to nodes that lie in many shortest paths between all other pairs of nodes. According to this criterion a bank is important when acting as middlemen in a flow of links. Let p_{ij} be the number of shortest paths between nodes i and j and p_{ikj} be the number of shortest path between nodes i and j passing through node k . Betweenness centrality is given by:

$$c_{(bw)_k} = \sum_i \sum_j \frac{p_{ikj}}{p_{ij}} \quad (21)$$

Ex ante measures also comprise input-output metrics (see [Aldasoro and Angeloni \(2014\)](#)), which are derived along the lines of the traditional Leontief input-output model. Banks transmit distress according to the coefficient of the input-output matrix, which in our case can be obtained by a transformation of the interbank exposure matrix. These measures allow for a more holistic approach to systemic importance by taking the balance sheet of the banking system as a starting point. Specifically, let the matrix \mathbf{X} represent the interbank exposure matrix, in which an element ij indicates exposure (through lending) of bank i to bank j . Then, the Rasmussen-Hirschman (RH) backward and forward indices are computed as follows:

$$h_{b_j} = \mathbf{i}' (\mathbf{I} - \mathbf{A})^{-1} \mathbf{i}_j \quad (22)$$

³⁹With this choice we cover the range of possible measures based on standard taxonomy (see for instance [Alves et al. \(2013\)](#)).

⁴⁰If one defines the geodesic (i.e. minimum distance) matrix as \mathbf{D} , then for a directed network in- and out-closeness can be defined analogously to degree measures, using \mathbf{D} instead of \mathbf{G}

$$h_{f_j} = \mathbf{i}'_j (\mathbf{I} - \mathbf{O})^{-1} \mathbf{i} \quad (23)$$

where \mathbf{A} is the interbank exposure matrix with each element expressed as a share of the borrowing (column) bank's total assets and \mathbf{O} is the interbank matrix with each element expressed as a share of the lending (row) bank's total assets⁴¹.

The input-output metrics allow for a distinction between distress coming from outside or within the interbank system. For the case in which one wishes to assess the potential distress that can come from interbank positions we use the so called “field of influence” (FoI). The column FoI captures the system effect of a unitary cut of interbank lending *to* bank j , whereas the row FoI assesses the systemic effect of a unitary cut of interbank lending *by* bank j . They read as follows:

$$f_{c_j} = \mathbf{i}' \left(\sum_{i \neq j} \mathbf{F}(i, j) \right) \mathbf{i} \quad (24)$$

$$f_{r_j} = \mathbf{i}' \left(\sum_{j \neq i} \mathbf{F}(i, j) \right) \mathbf{i} \quad (25)$$

where $\mathbf{F}(i, j) = \mathbf{b}_i \mathbf{b}'_j$ is the field of influence matrix, with \mathbf{b}_i and \mathbf{b}'_j denoting respectively the i^{th} column and the j^{th} row of the Leontief inverse defined above. The average of the two measures can be combined into a total field of influence.

Finally, the “total linkage effect” measures the cost in terms of total assets of the system of a complete cut-off of a given bank from the interbank system (see [Aldasoro and Angeloni \(2014\)](#) for details on the formula).

E Additional results for baseline scenario

E.1 Balance sheet characteristics and systemic importance ranking

⁴¹For details on the derivations see [Aldasoro and Angeloni \(2014\)](#), which perform a normalization to the measures to express them relative to the mean of the system, set equal to unity such that banks with an index higher (lower) than 1 are (not) systemically important. Furthermore, the distance of the index from 1 provides an idea of relative importance. The matrix $(\mathbf{I} - \mathbf{A})^{-1}$ is normally referred to as the Leontief inverse.

	Banks																			
	1	2	3	4	5	6	7	8	9	10	11	12	13	14	15	16	17	18	19	20
Cash	56.9	53.6	48.7	30.5	57.0	46.6	36.4	20.5	22.9	25.8	3.9	14.3	12.7	10.7	6.8	12.1	12.9	6.7	7.3	7.7
Non-liquid assets	606.0	807.3	529.2	211.9	838.3	296.6	250.8	428.7	284.9	40.7	8.2	252.8	24.0	111.1	88.9	51.8	63.1	111.1	100.0	11.6
Interbank lend.	92.3	0.0	74.8	144.7	0.0	175.8	153.6	0.0	64.6	234.5	46.9	44.7	138.0	0.0	0.0	62.1	59.0	0.0	0.0	66.7
Interbank borr.	130.7	234.9	117.2	29.1	244.3	0.0	19.8	196.2	117.5	0.0	0.0	145.8	31.7	4.8	19.7	0.0	0.0	40.8	25.3	0.0
Total Assets (A)	755.2	860.9	652.7	387.1	895.3	519.0	440.8	449.2	372.5	301.0	59.0	311.8	174.7	121.8	95.7	126.0	135.0	117.8	107.3	86.0
Equity	55.6	90.0	48.5	53.0	81.0	53.0	57.0	48.0	26.0	43.0	20.0	23.0	16.0	10.0	8.0	5.0	6.0	10.0	9.0	9.0
Leverage	13.6	9.6	13.5	7.3	11.1	9.8	7.7	9.4	14.3	7.0	3.0	13.6	10.9	12.2	12.0	25.2	22.5	11.8	11.9	9.6
Liquid assets/A (%)	19.8	6.2	18.9	45.3	6.4	42.9	43.1	4.6	23.5	86.5	86.2	18.9	86.3	8.8	7.1	58.9	53.3	5.7	6.8	86.5
Interbank lend./A (%)	12.2	0.0	11.5	37.4	0.0	33.9	34.8	0.0	17.4	77.9	79.6	14.3	79.0	0.0	0.0	49.3	43.7	0.0	0.0	77.6
Interb. borr./Liab. (%)	18.7	30.5	19.4	8.7	30.0	0.0	5.1	48.9	33.9	0.0	0.0	50.5	20.0	4.3	22.5	0.0	0.0	37.9	25.7	0.0
Nla/Dep. (%)	106.5	150.6	108.7	69.5	147.1	63.6	68.9	209.1	124.4	15.8	20.9	176.8	18.9	103.8	130.7	42.8	48.9	165.8	137.0	15.0
Nla/Equity (%)	1090.7	897.0	1092.1	399.9	1035.0	559.6	440.0	893.1	1095.9	94.7	40.8	1099.3	149.9	1111.1	1111.1	1035.2	1051.0	1111.1	1111.1	128.8
Interb. lend./Equity (%)	166.1	0.0	154.3	273.0	0.0	331.7	269.4	0.0	248.6	545.3	234.7	194.3	862.8	0.0	0.0	1242.8	984.0	0.0	0.0	741.2

Table 4: Optimal balance sheet items - Baseline setting

Centrality		Network																			
		1	2	3	4	5	6	7	8	9	10	11	12	13	14	15	16	17	18	19	20
In-degree	RAS	7	1	8	9	2	16	3	4	10	17	11	12	13	5	6	18	19	14	20	15
	CMA	5	3	6	7	8	16	1	2	9	17	10	11	12	13	14	18	19	4	20	15
	RMA	2	3	5	10	6	16	7	1	8	17	13	9	14	15	11	18	19	4	20	12
Out-degree	RAS	6	15	7	8	16	1	17	18	9	2	10	11	12	19	20	3	4	13	5	14
	CMA	11	15	5	6	16	12	17	18	1	7	2	3	4	19	20	13	14	8	9	10
	RMA	6	15	7	4	16	8	17	18	11	1	5	12	13	19	20	9	2	10	14	3
In-out degree	RAS	1	15	2	3	16	10	17	18	4	11	5	6	7	19	20	12	13	8	14	9
	CMA	12	8	9	10	15	16	1	2	3	13	4	5	6	17	18	19	20	7	14	11
	RMA	1	12	3	4	14	15	16	6	7	8	9	10	13	19	18	17	11	5	20	2
Closeness-in	RAS	10	14	8	3	15	16	12	13	9	17	6	11	4	1	2	18	19	7	20	5
	CMA	13	4	11	9	15	16	2	3	12	17	10	14	8	5	7	18	19	1	20	6
	RMA	14	8	10	4	12	16	2	3	17	15	9	13	11	1	18	19	5	20	6	
Closeness-out	RAS	8	15	7	12	16	13	17	18	4	14	9	1	11	19	20	3	5	6	2	10
	CMA	11	15	6	10	16	14	17	18	3	9	2	4	1	19	20	12	13	7	8	5
	RMA	12	15	8	7	16	9	17	18	6	13	11	4	10	19	20	2	1	3	14	5
Closeness-in-out	RAS	14	19	10	3	20	15	17	18	6	16	12	2	8	1	4	7	13	9	5	11
	CMA	14	8	11	12	20	19	4	5	6	15	3	7	1	9	16	17	18	2	13	10
	RMA	16	12	11	7	18	14	5	10	1	19	15	9	13	17	3	8	4	2	20	6
Betweenness	RAS	4	5	6	1	7	8	9	10	11	12	13	2	14	15	16	17	18	19	20	3
	CMA	9	10	3	8	11	12	13	14	2	15	4	7	6	16	17	18	19	1	20	5
	RMA	1	10	7	4	11	12	13	14	5	15	9	3	8	16	17	18	19	6	20	2
Eigenvector (left)	RAS	6	2	8	13	1	16	4	3	7	17	10	5	12	15	14	18	19	9	20	11
	CMA	5	9	3	12	13	14	10	6	1	15	4	16	8	11	17	18	19	2	20	7
	RMA	11	3	7	10	5	16	1	2	14	17	12	13	6	8	4	18	19	9	20	15
Eigenvector (right)	RAS	7	15	9	3	16	2	17	18	11	1	6	14	4	19	20	12	8	10	13	5
	CMA	3	8	5	9	10	11	12	13	7	14	4	15	1	16	17	18	19	6	20	2
	RMA	12	15	5	3	16	6	17	18	10	4	7	11	14	19	20	1	13	9	8	20

Table 5: Systemic importance ranking by network centrality measures, bank and network - Baseline setting

IO measure	Network	Banks																			
		1	2	3	4	5	6	7	8	9	10	11	12	13	14	15	16	17	18	19	20
R.H. Backward	RAS	13	9	12	14	8	16	6	4	7	17	2	3	11	15	10	18	19	1	20	5
	CMA	12	8	9	14	11	16	7	5	4	17	2	6	10	15	13	18	19	1	20	3
	RMA	12	10	13	14	8	16	5	4	9	17	3	2	7	15	11	18	19	1	20	6
R.H. Forward	RAS	13	15	14	9	16	10	17	18	11	3	1	12	4	19	20	7	6	8	5	2
	CMA	13	15	12	9	16	10	17	18	11	4	1	14	3	19	20	8	7	6	5	2
	RMA	13	15	14	9	16	10	17	18	12	1	2	11	5	19	20	7	6	8	4	3
Row FoI	RAS	6	17	9	3	18	2	19	20	12	1	7	14	4	15	16	10	8	13	11	5
	CMA	1	18	2	3	17	11	19	20	7	9	5	14	6	15	16	13	12	4	10	8
	RMA	13	17	5	9	18	3	19	20	14	1	4	6	7	15	16	10	11	8	12	2
Column FoI	RAS	10	2	6	13	1	16	4	3	7	20	9	5	12	15	14	17	18	8	19	11
	CMA	11	6	3	14	5	16	1	2	4	20	12	7	13	15	10	17	18	9	19	8
	RMA	9	6	7	12	2	16	1	5	10	20	11	3	8	15	14	17	18	4	19	13
Total FoI	RAS	15	2	5	10	1	11	3	4	8	7	12	6	13	20	19	17	16	9	18	14
	CMA	5	11	1	8	6	17	2	4	3	14	9	13	12	20	16	19	18	7	15	10
	RMA	14	8	6	13	4	12	3	7	15	1	9	2	11	20	19	16	17	5	18	10
Total Linkage	RAS	4	2	7	14	1	12	6	5	9	3	11	8	13	20	19	17	16	10	18	15
	CMA	3	5	1	14	6	13	8	7	2	4	11	15	12	20	19	17	16	9	18	10
	RMA	6	2	10	12	1	11	5	8	14	3	13	7	9	20	19	17	16	4	18	15

Table 6: Systemic importance ranking by input-output measures, bank and network - Baseline setting

E.2 Additional results on Shapley value

Figure 7 plots the Shapley value versus bank characteristics for the RAS network. Results point to a strong connection with total assets as discussed in the main body of the paper. The connection to other measures is rather weak. Figure 8 on the other hand sheds light on the extent to which systemic importance and systemic risk measures deliver a consistent ranking of banks by plotting the Shapley value versus the six different input-output measures considered⁴². The bottom line is that there is no apparent connection between the ranking provided by the two types of measures.

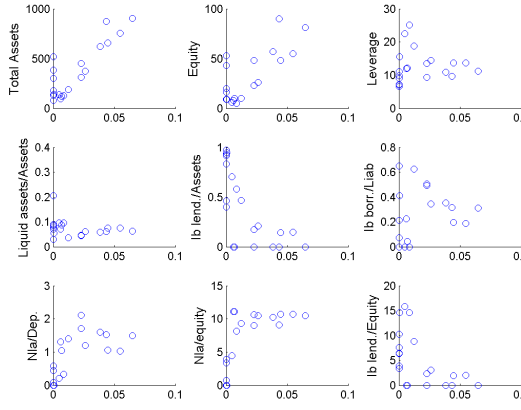


Figure 7: SV vs. bank characteristics (RAS)

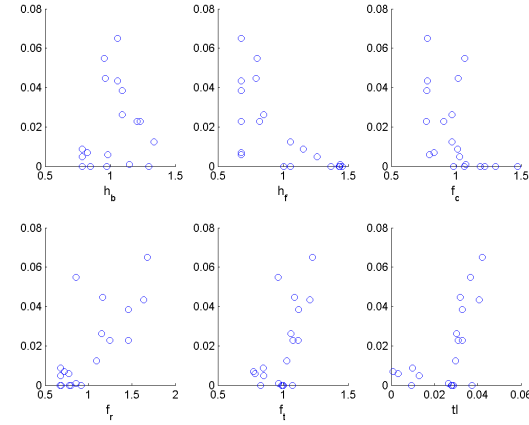


Figure 8: SV vs. IO measures (RAS)

E.3 Systemic importance measures and bank characteristics

The relationship between input-output metrics and bank characteristics depends on the measure considered⁴³. Figure 9 and Figure 10 present the results for the backward and forward indicators respectively, both for the RAS network. The former shows a strong relationship to interbank borrowing as a share of liabilities and also a positive relationship with non-liquid assets as a share of deposits, whereas the latter shows a strong relationship with interbank lending as a share of assets. The strong connections both indicators show with some balance sheet characteristics are not particularly surprising as they stem from their very construction.

⁴²Results for the comparison between network centrality and Shapley values deliver the same message and are omitted for the sake of space and are available upon request. The same applies to results for the other networks.

⁴³Results are only presented when considering the RAS network. For other networks results are largely unchanged and are available upon request. Furthermore, for space considerations we leave out the results pertaining to network centrality measures versus balance sheet characteristics. The results show slightly more differences between different types of networks (RAS, CMA, RMA) but no indicator shows a particularly strong relationship to balance sheet items. Results are available upon request.

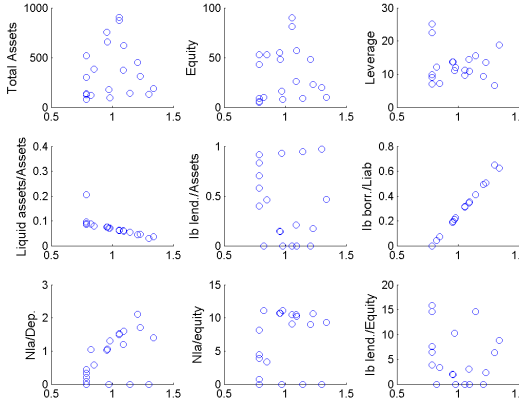


Figure 9: RH backward index (\bar{h}_b) vs. bank characteristics (RAS)

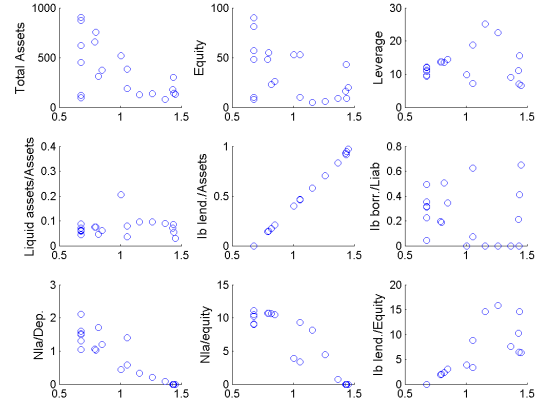


Figure 10: RH forward index (\bar{h}_f) vs. bank characteristics (RAS)

For other measures this connection is not as strong. [Figure 11](#) and [Figure 12](#) present the results for the total field of influence and the total linkage effect, pointing to a relatively strong connection to total assets only.

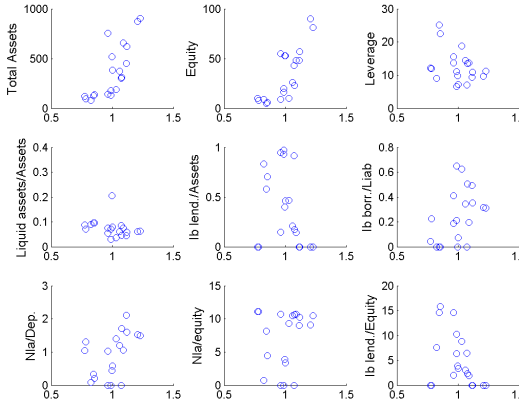


Figure 11: Total Field of Influence (FoI)

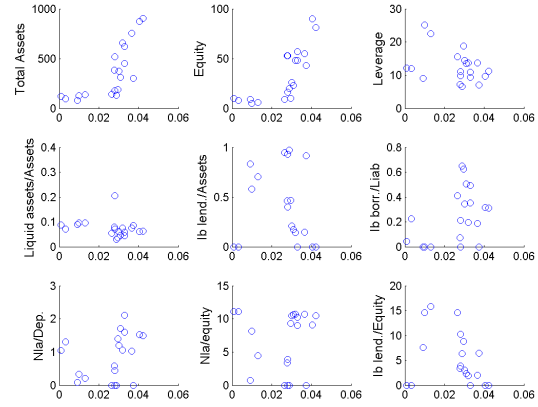


Figure 12: Total Linkage Effect

F Model Comparison

In this section we compare the results from different models to illustrate some differences. We perform a policy analysis in the same fashion as in the main body of the paper. For all models considered the interbank matrix was obtained by means of the RAS algorithm, and the shock simulation involves 1000 realizations of the shock vector. We consider the following three alternative models:

- **Model 1:** this model is the one presented in the main body of the paper, featuring risk averse banks and the interaction of fire sales and network externalities.
- **Model 2:** this model has risk neutral instead of risk averse banks, hence the objective function is linear and simply given by utility of expected profits, which in this case is equal to expected utility of profits. The constraints remain the same, and fire sales and interbank contagion are also kept. It is worth noting that in this model there are no banks that participate on both sides of the market simultaneously, i.e. they are either borrowers or lenders.
- **Model 3:** this model is similar to *Model 1* but it eliminates the fire sales channel. Non-liquid assets are no longer a choice variable of banks and are instead calibrated by the values banks would have chosen if given the chance. Once a shock hits banks cannot sell the assets and the transmission of distress takes place only through the interbank channel.
- **Model 4:** this model is a small variation of *Model 3*. In particular, we set the risk aversion parameter to $\sigma = 0$.

Results from the comparison exercise are summarized in [Table 7](#), which presents the effects of changes in the liquidity and equity requirements on systemic risk, interbank lending over total assets and non-liquid assets over equity.

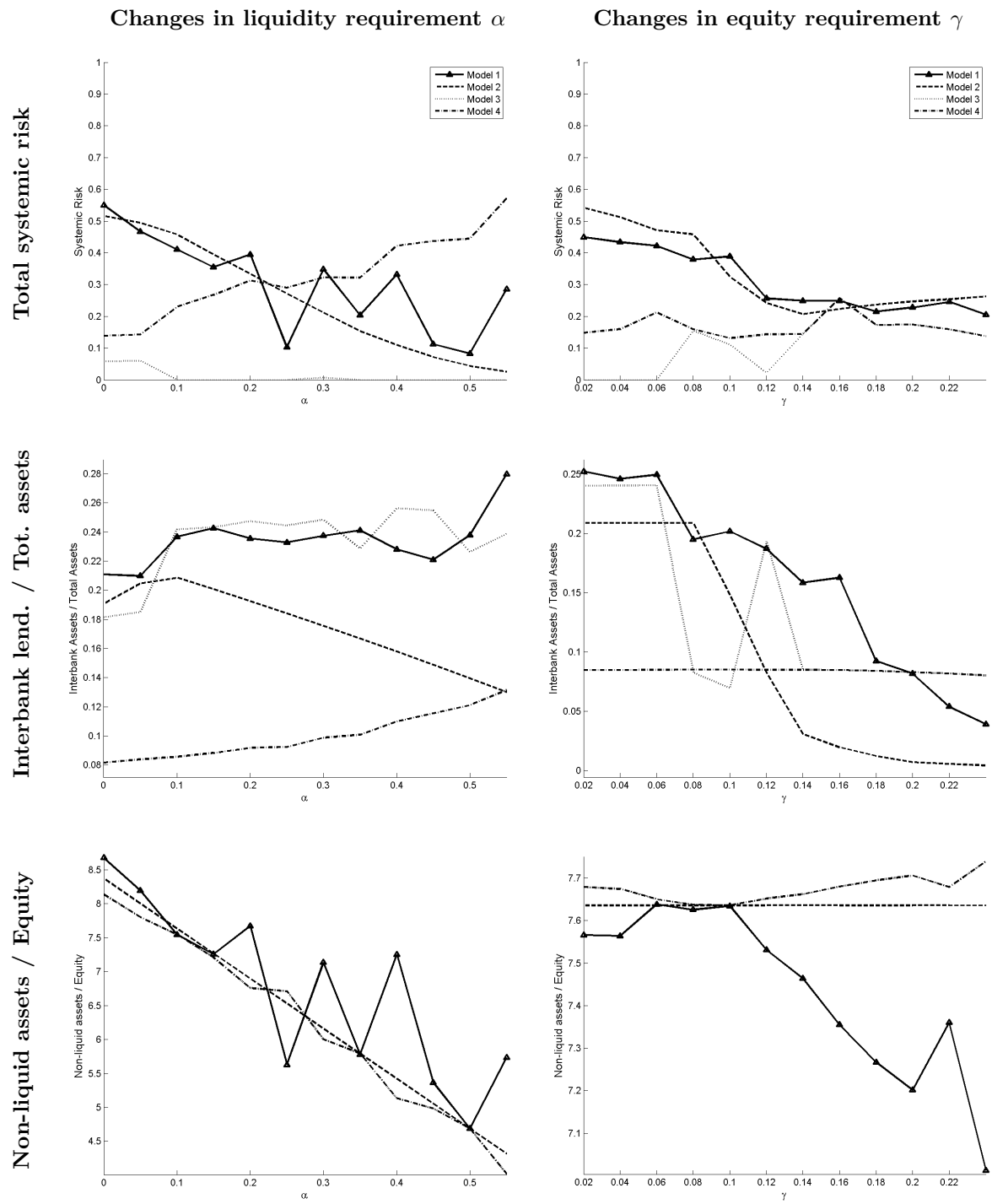


Table 7: Model Comparison

G Additional results for comparative static analysis

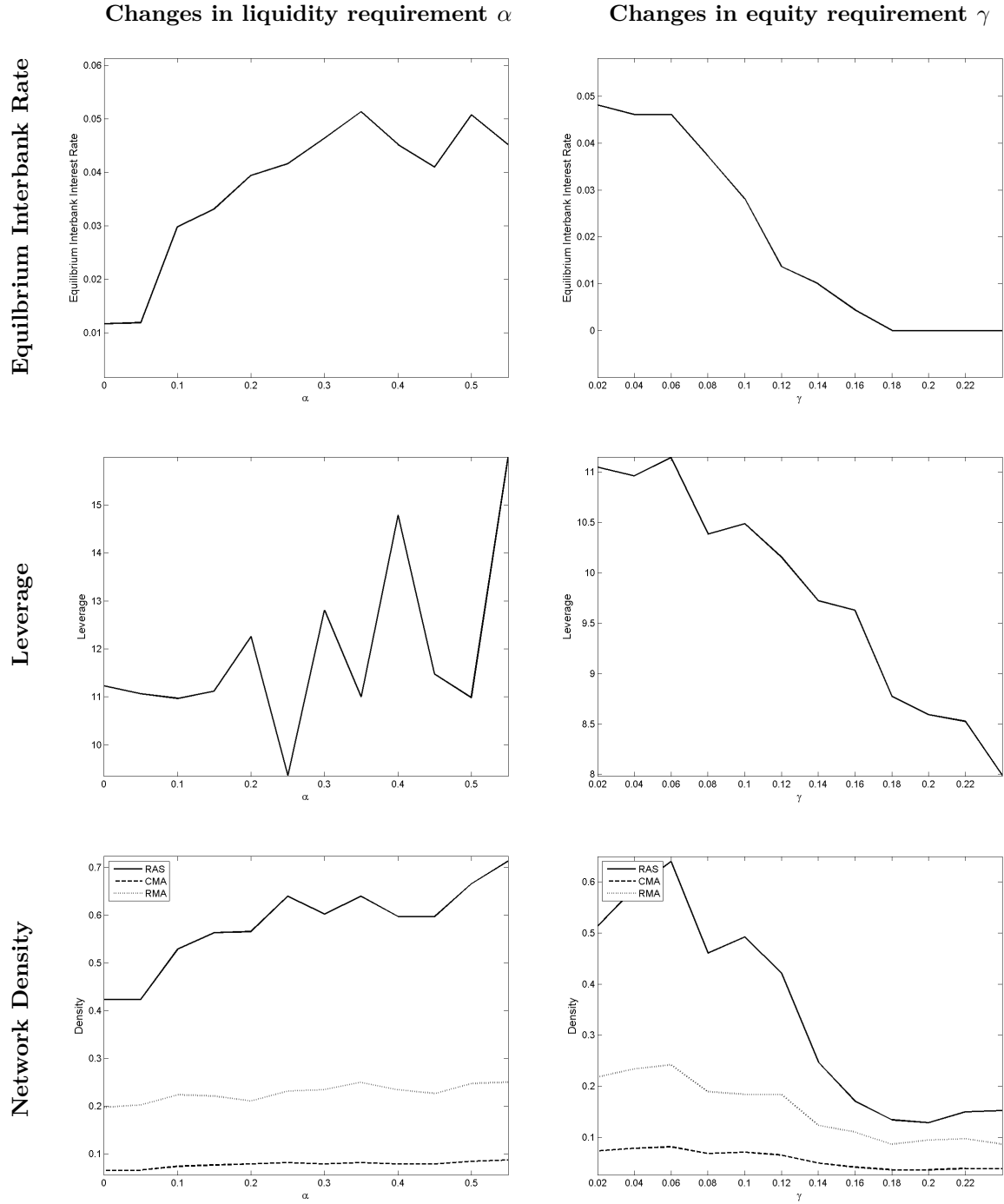
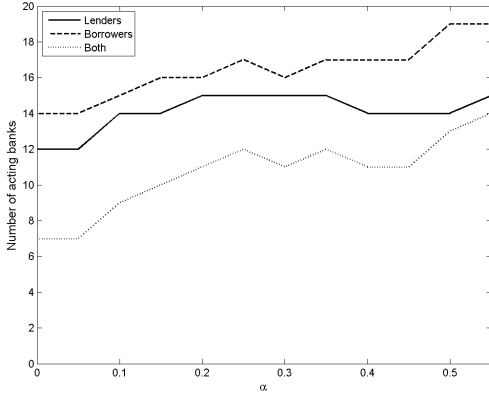
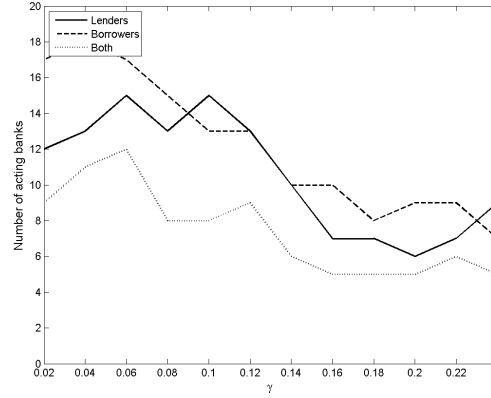


Table 8: Additional results from policy analysis



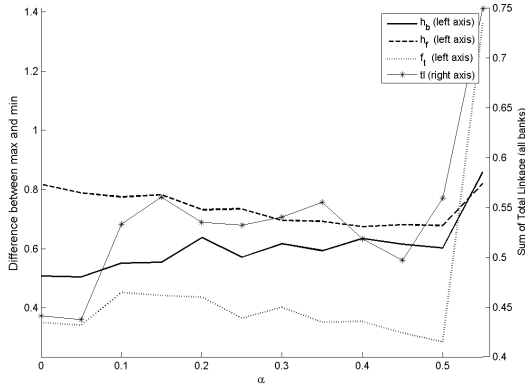
(a) Changes in LR (α)



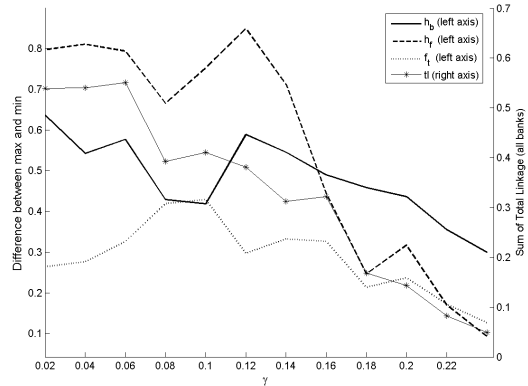
(b) Changes in ER (γ)

Figure 13: Number of active banks in interbank market for different values of α and γ

We also use some input-output measures to obtain further insights. The distance of the normalized indices to 1 provides an idea of relative importance, hence the difference between maximum and minimum values provides insights on whether the system is becoming more or less homogenous (decreasing or increasing difference respectively). Additionally, the sum total linkage effect for all banks provides a quantification of the loss of system-wide assets caused by a collapse of the entire interbank market. Figure 14 presents results for the two policy experiments. For changes in the liquidity requirement (panel 14a) all lines stay rather flat, with a couple of exceptions at the right end of the spectrum. On the other hand, changes in the equity requirement (panel 14b) deliver a completely unambiguous message: all indicators are decreasing, pointing to a more homogenous banking system and less potential damage of interbank market collapses.



(a) Changes in LR (α)



(b) Changes in ER (γ)

Figure 14: IO measures: max - min (\bar{h}_b , \bar{h}_f , \bar{f}_t , left axis) and sum over all banks (tl , right axis)

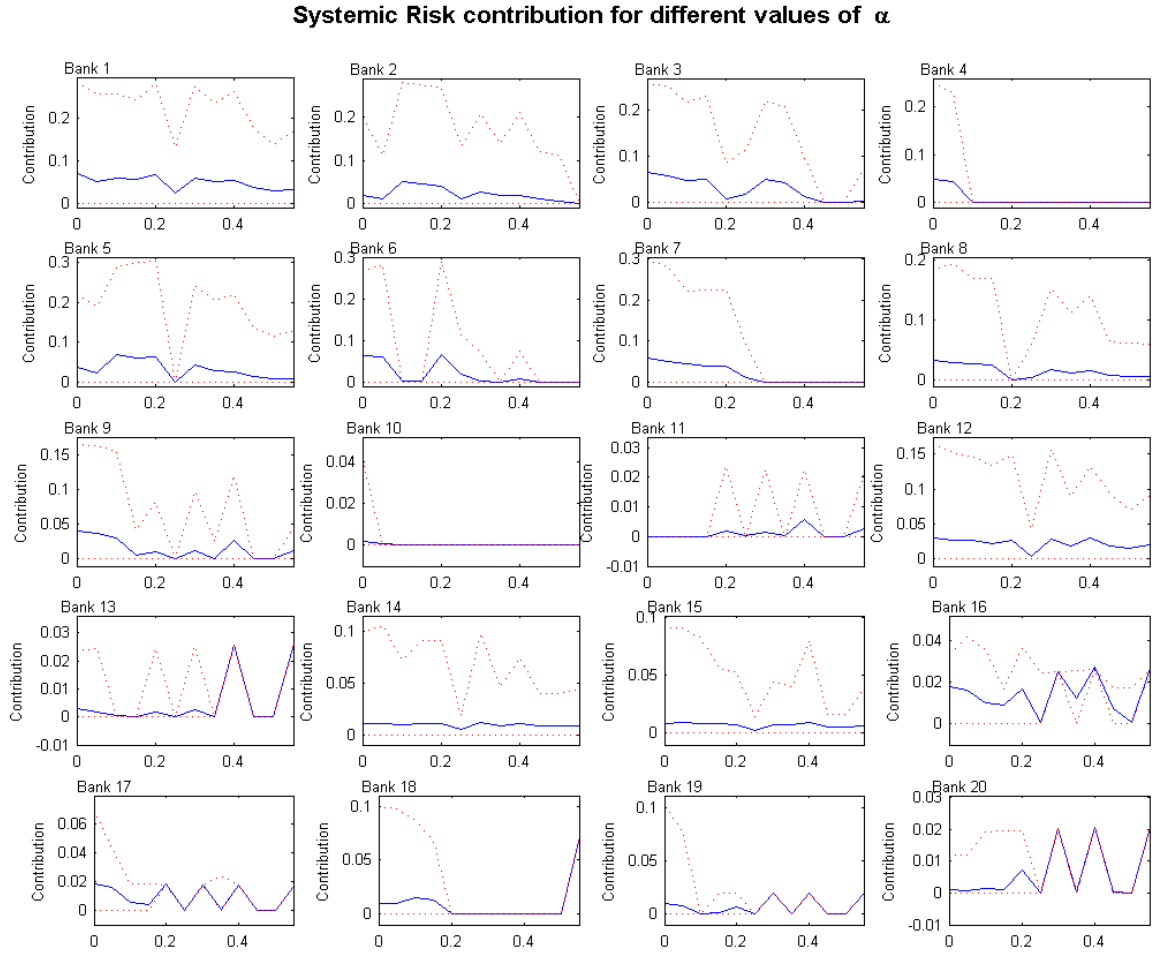


Figure 15: Contribution to systemic risk (Shapley Value) by bank for different values of α and for the RAS network

Systemic Risk contribution for different values of γ

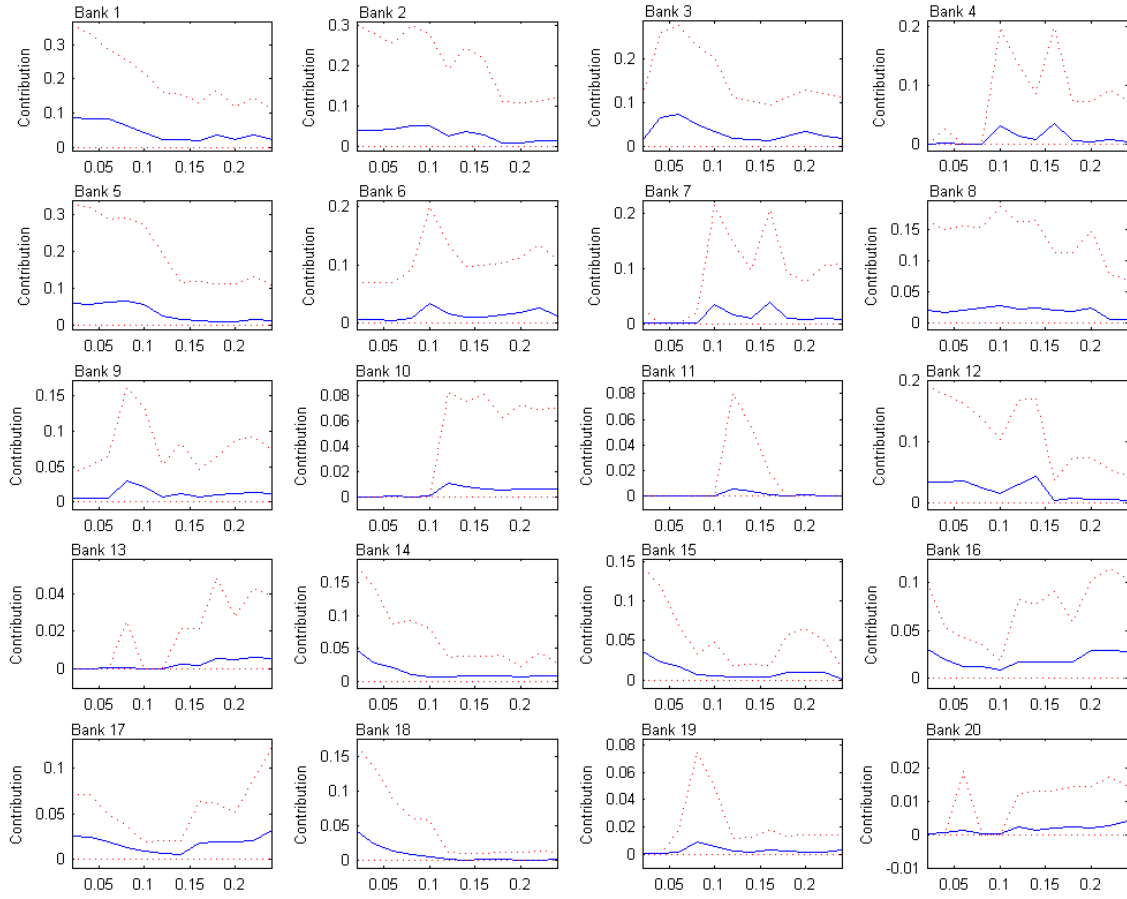


Figure 16: Contribution to systemic risk (Shapley Value) by bank for different values of γ and for the RAS network

Systemic Risk contribution for different values of α

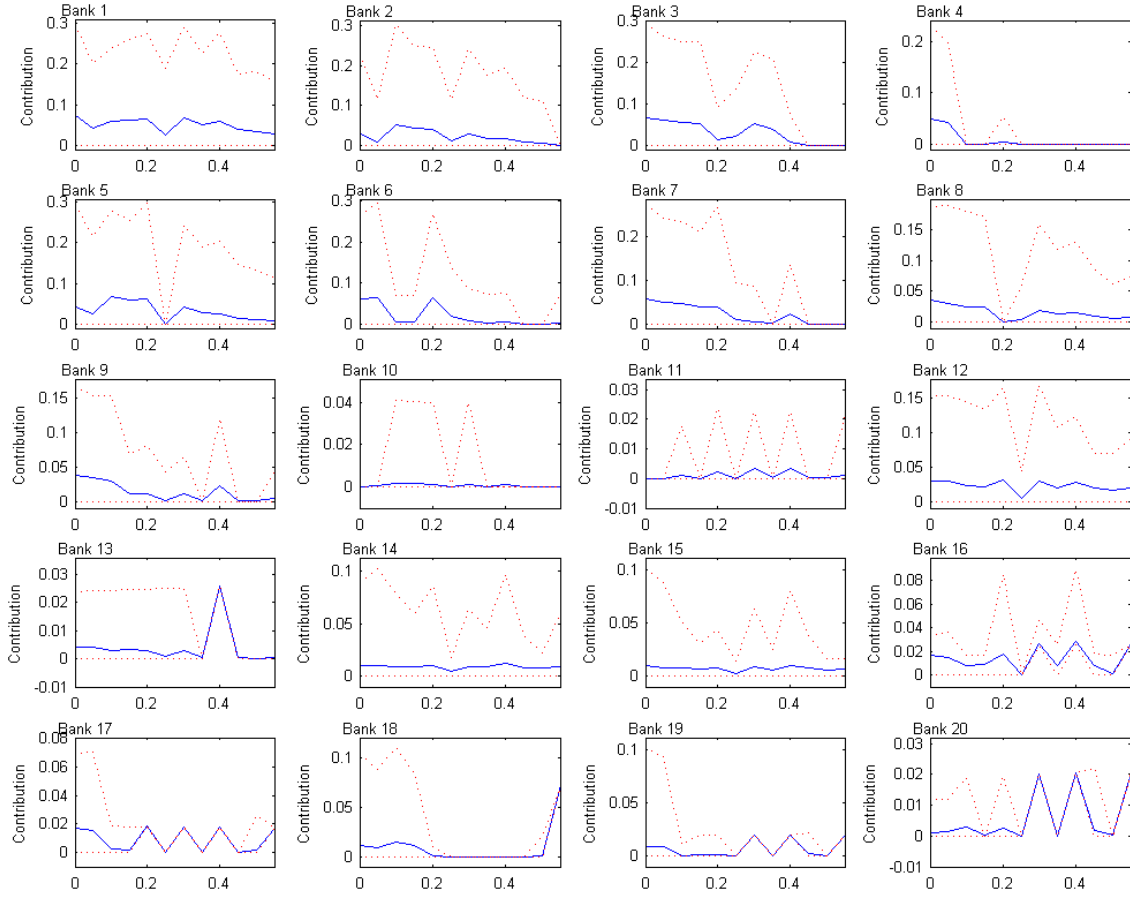


Figure 17: Contribution to systemic risk (Shapley Value) by bank for different values of α and for the CMA network

Systemic Risk contribution for different values of γ

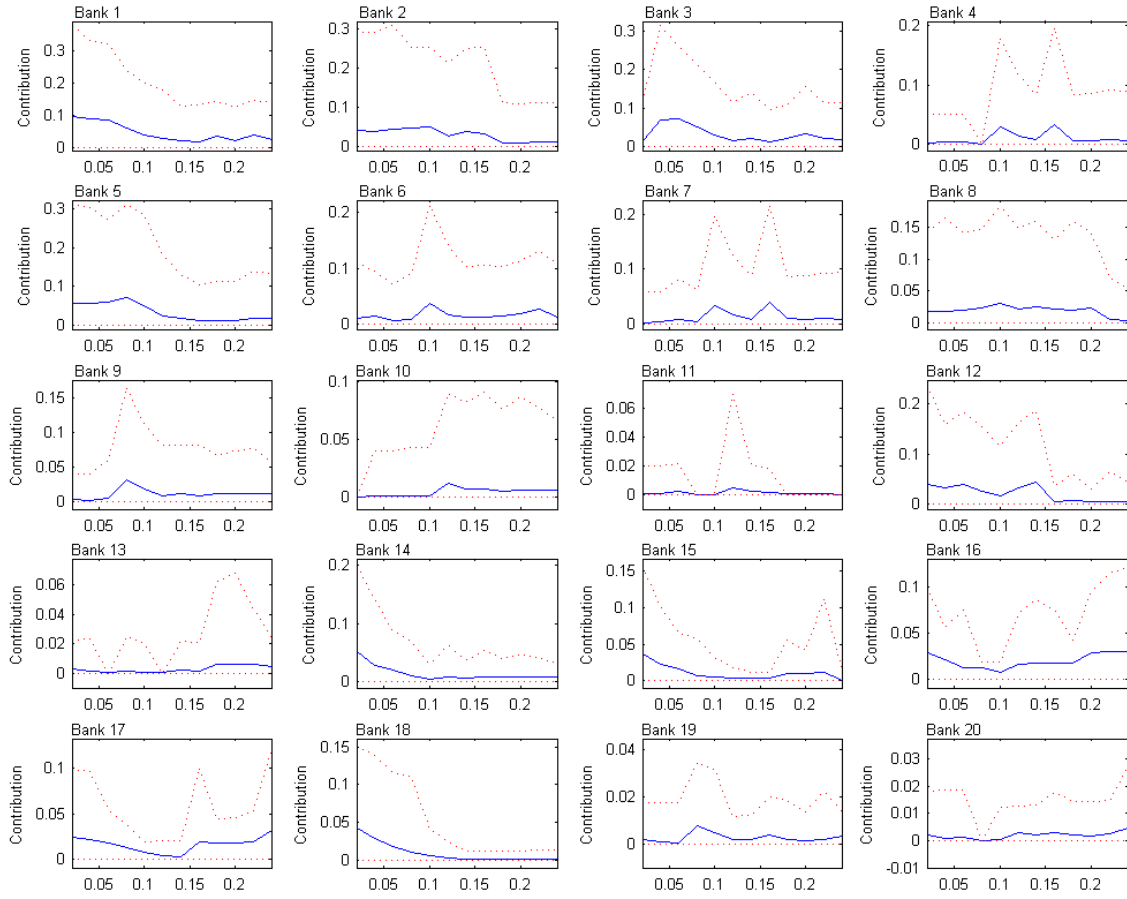


Figure 18: Contribution to systemic risk (Shapley Value) by bank for different values of γ and for the CMA network

Systemic Risk contribution for different values of α

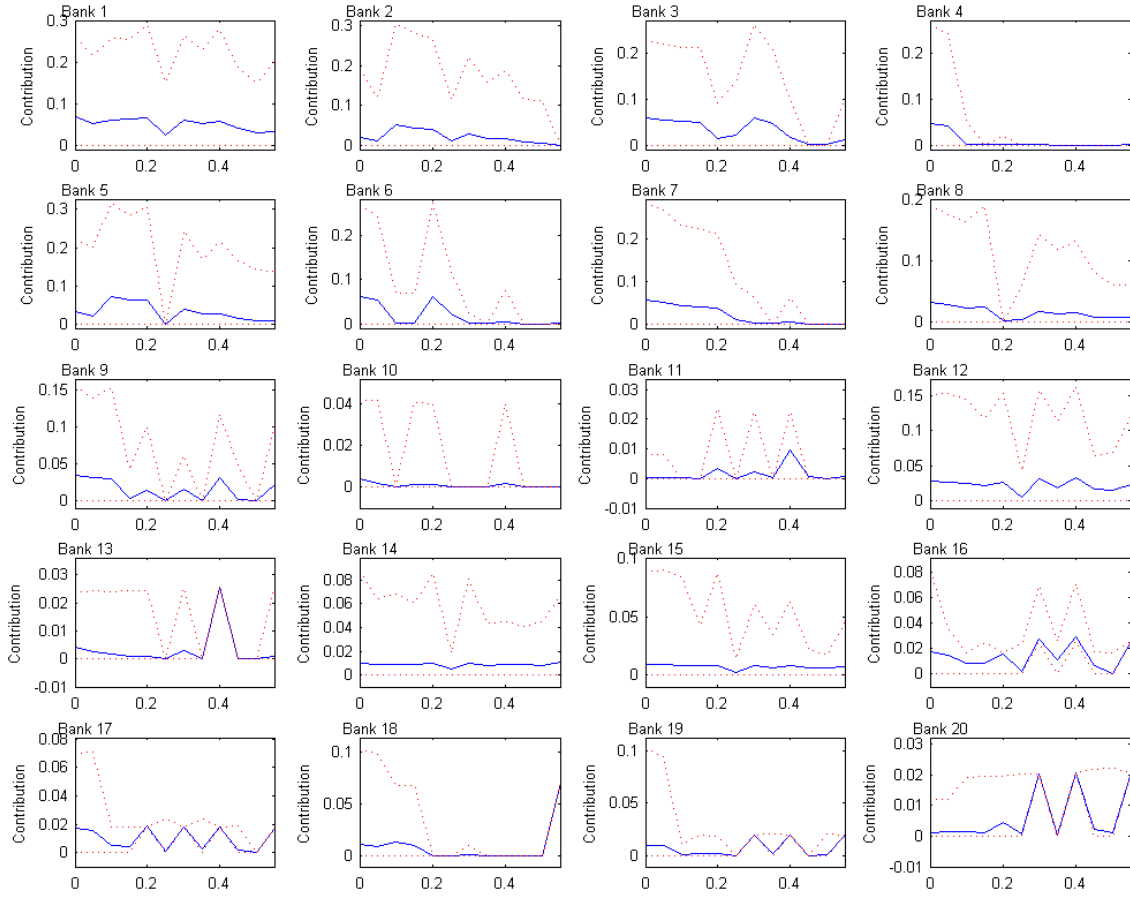


Figure 19: Contribution to systemic risk (Shapley Value) by bank for different values of α and for the RMA network

Systemic Risk contribution for different values of γ

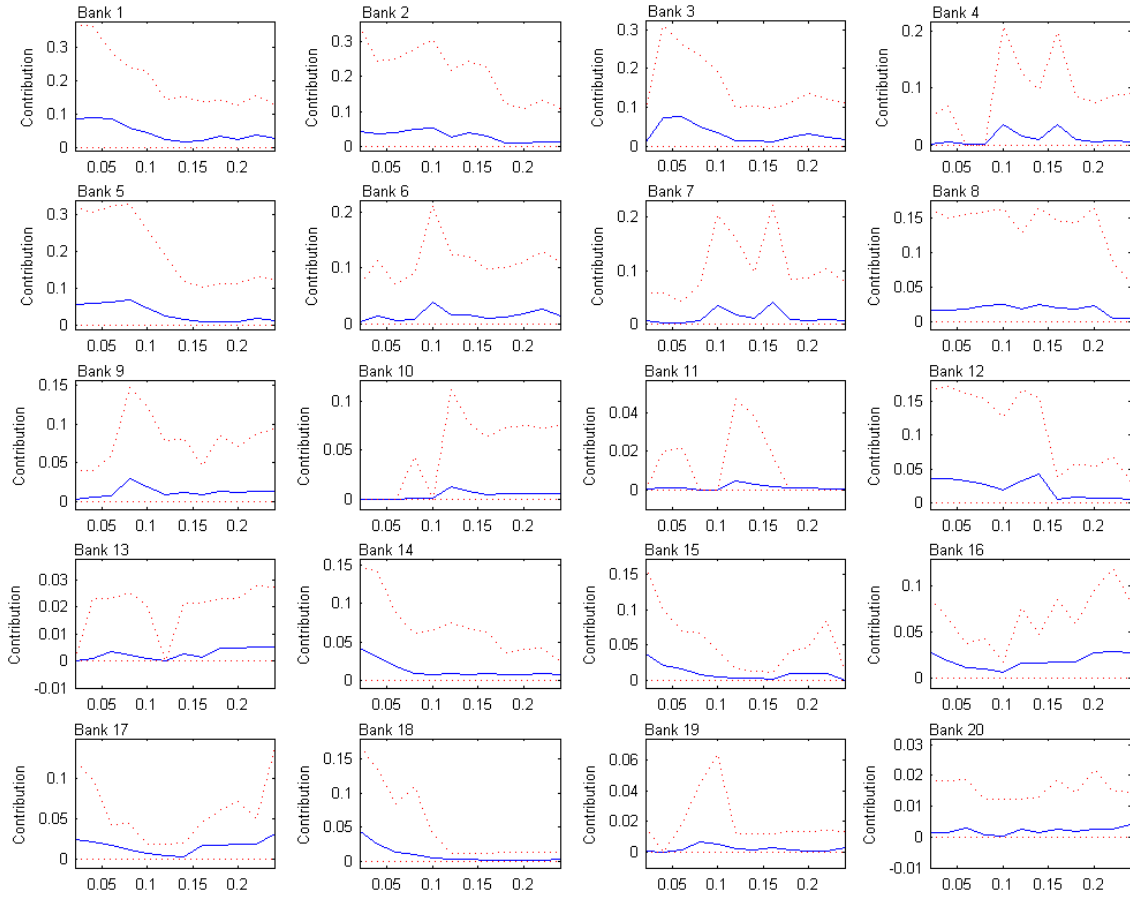


Figure 20: Contribution to systemic risk (Shapley Value) by bank for different values of γ and for the RMA network